AGRICULTURAL ENGINEERING SOLUTIONS

ISSN: 2181-399X Volume 3, Issue 3, 2023

THEORETICAL RESEARCH OF CONSTANT VELOCITY MOVEMENT OF THE BASE PLATE THROUGH WORKING SHAFT PAIRS

T. Sultanov[1], Z. Rakhimova[2], E. Toshmatov[1]

[1]"Tashkent Institute of Irrigation and Agricultural Mechanization Engineers" National Research University, 39, Street Kari Niyaziy, Tashkent, 100000, Uzbekistan,
[2]Tashkent chemical – technological Institute, A.Navoiy street 32, 100011, Tashkent, Uzbekistan

Abstract: In this scientific article it is described that, the case where the base plate on which the flat material is suspended exits the coverage area of the shaft pairs covered with the first working elastic material and the shaft pairs covered with the second working elastic material hit the coverage area, when the forces acting on the shafts are under potential forces. For a mechanical system under potential forces, Lagrange's second-order motion equations are formulated. Solutions of the formulated equations were obtained and theoretically studied.

Keywords: flat material, coverage angle, shaft pair, base plate, gravity, gravitational force

Introduction. Today, the main thing in improving the machining processes in shaft machines processing flat materials (including many semi-finished products) is to study and solve the problem of mutual coverage between shaft [1].

Contact zone has a major effect on machine stiffness. For an accurate calculation, the contact stiffness should be known. This paper presents the approach to determine the elastic characteristic of the contact layer formed by two rough surfaces [2]. Proposes to use a plastic and composite material of a flexible element, which acts as sliding support instead of a detailed rolling bearing, which provides a smooth rotational movement of the guide roller mechanism, which performs the rotational movement of the conveyer belt [3].

New analytical dynamic models have been developed for roller machines used in industry [4], [5].

The presents the results of experimental studies obtained by determining the influence of multilayer wet leather semi-finished products with monsoons under squeezing on the amount of the moisture extracted. Mathematical dependences of the amount of the moisture extracted, for each layer of a five-layer wet leather semi-finished product on the feed rate between the squeeze rollers and the roller pressure were obtained. Experimental research is of scientific and practical importance for the development of a technological process for extracting moisture from wet leather semi-finished products used in the tannery, since the quality of the extraction affects the quality of subsequent technological operations, such as leather shaping and splitting [6]. The results of experimental studies are presented in the paper by determining the effect of the amount of water extracted from the leather semi-finished products under their simultaneous squeezing between rotating working rollers. A mathematical dependence of the amount of squeezed out water from wet leather semi-finished products under various pressures of the working rollers and the feed rate on the number of layers of leather semi-finished product with monsoons was obtained [7]. Papers are devoted to solutions of contact interaction in two-roll modules. They obtained mathematical models of roll contact curves, friction stresses and contact stress distribution patterns. Examines the movement of a mechanical machining machine on a flat material between a pair of shafts with an elastic coating and a base plate. Using Lagrange's 2-Round motion equations, the motion differential equations of a pair of shafts with an elastic coating are structured. Graphs were built and analyzed on the basis of solutions of the differential equations of motion.

For non-nogolonomic systems of mechanical systems, the equations of motion are derived and analyzed. In this work the problem of selecting the orientation surface appearance when smooth material is uniformly transferred to the machining zone of the flat material, i.e. between the working shafts, has been considered and studied. The movement of the flat material in the processing zone through the conveyor is studied. The laws of dynamics and numerical methods were used to determine the appearance of the transferring surface.

Materials and methods. We have developed a line for the transportation and machining of flat material, ie leather semi-finished products. This technological line has three main working zones, where various technological processes are carried out using pairs of working shafts and base plates. In the case under consideration, in order for the vertical shaft machine that mechanically processes the flat material to operate at the required level, we need to ensure that the flat material hanging base plate moves at a constant speed. Consider the following issue.

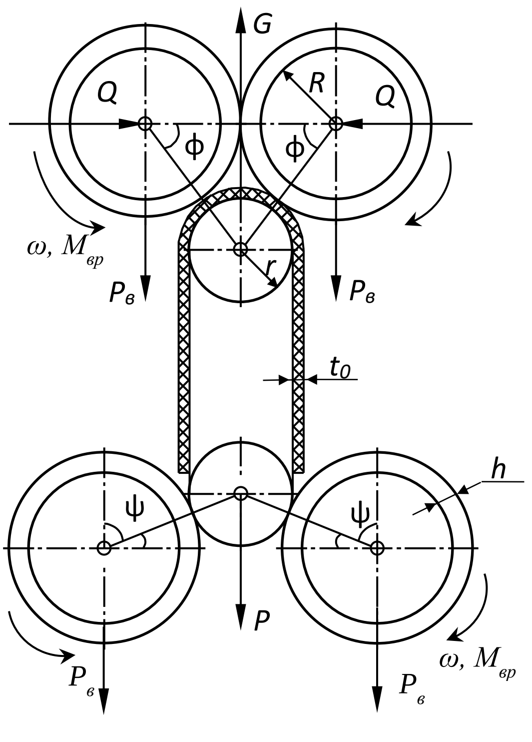

Figure 1. Scheme of the base plate leaving the coverage area of the first working elastic shaft pairs and hitting the coverage area of the second working elastic shaft pairs

To do this, follow this process below; the base plate on which the flat material is hung comes out of the coverage area of the shaft pairs covered with the first working elastic material, a pair of shafts covered with a second working elastic material hit the coverage area (figure 1), state, how fast the base plate moves when the forces acting on the shafts are under the influence of potential forces are considered. To do this, using Lagrange's type 2 equations, we formulate the equations with respect to the quantities we need.

First, we determine the degree of freedom of the system under consideration (according to Figure 1). In this case, the degree of freedom is three because the pairs of shafts covered with an elastic material move in a straight parallel at the exit of the base plate from the coverage area. Since the base plate is in forward motion along the chain, the degree of freedom in this case is equal to 2. When the base plate hits a pair of shafts lined with a highly working elastic material, the shafts are in rotational motion and in this case the degree of freedom is equal to one. This means that the degree of freedom of the system we are looking at is equal to 6. In that case the generalized coordinates will also be 6. These are: $x_1 = q_1, y_1 = q_2, \psi = q_3, x_2 = q_{4,} y_2 = q_5, \varphi = q_6$.

We formulate the equations of motion for the case where the base plate on which the flat material is suspended exits the coverage area of the shaft pairs covered with the first working elastic material and the second working shaft pair hits the coverage area. To do this, we first calculate the kinetic energy of the base plate and the elastically coated shafts. In this case, the base plate on which the flat material is suspended moves forward throughout the system, and its kinetic energy is expressed as follows.

$$T_1 = \frac{M\vartheta_c^2}{2} = \frac{1}{2}m_1\dot{y}^2 = \frac{1}{2}m_1\left(\dot{y}_1^2 + \dot{y}_2^2\right), \tag{1}$$

In this $T_1 -$ kinetic energy of the base plate,

$m_1 -$ chain, mass of base plate and flat material.

Given the bottom shaft pair moves in a straight parallel at the exit from the coverage area of the base plate on which the flat material is hung (1-figure) and their kinetic energy is written as follows.

$$T_2 = T_3 = \frac{M\vartheta_c^2}{2} + I_{Cz}\frac{\omega^2}{2} = \frac{1}{2}m_2\dot{x}_1^{\,2} + \frac{1}{2}J_{Cz}\omega^2, \tag{2}$$

In this $T_2, T_3 -$ kinetic energy of lower shafts.

$m_2 = m_3 -$ mass of bottom shafts, $J_{Cz} -$ the moment of inertia about the axis passing through the center of mass of the shaft perpendicular to the plane of motion, $\omega -$ angle speed. In the case, the moment of inertia of the shaft is equal $J_{Cz} = \frac{m_2 R^2}{2}$, where $R -$ the radius of shafts.

When the base plate, on which the flat material is hung, hits the coverage area of the shafts above the second working elastic, the shafts move in a slow rotational motion. In this case, the kinetic energy of the above shafts is expressed as follows:

$$T_4 = T_5 = I_z\frac{\omega^2}{2} \tag{3}$$

In this $T_4, T_5 -$ kinetic energy of upper shafts. $m_4 = m_5 -$ mass of upper shafts.

$J_z -$ moment of inertia about the axis of rotation of the shaft, $\omega -$ angle speed. In the case, the moment of inertia of the shaft relative to the axis of rotation according to the Huygens-Steiner theorem is equal to $J_z = \frac{3m_4 R^2}{2}$. In this $R -$ radius of shafts.

Now and connect the coordinates x and y with the coverage angle ψ for the lower shafts, in which case we have the following expression.

$$\begin{aligned} x_1 &= \left(R + r + h_0\right)\cos\psi, \\ y_1 &= \left(R + r + h_0\right)\sin\psi, \end{aligned} \tag{4}$$

In this $R -$ radius of shafts, $r -$ the radius of the "nose" of the base plate, $h_0 -$ monson thickness of shafts. If we derive the expression from (4), it is equal to the following.

$$\begin{aligned} \dot{x}_1 &= -\left(R + r + h_0\right)\dot{\psi}\sin\psi, \\ \dot{y}_1 &= \left(R + r + h_0\right)\dot{\psi}\cos\psi. \end{aligned} \tag{5}$$

Now and for the upper shaft pairs, we connect the coordinates x and y with the coverage angle φ, in which case we have the following expression.

$$\begin{aligned} x_2 &= \left(R + r + h_0 + t_0\right)\cos\varphi, \\ y_2 &= \left(R + r + h_0 + t_0\right)\sin\varphi, \end{aligned} \tag{6}$$

In this $R-$ the radius of shafts, $r-$ the radius of the "nose" of the base plate, $h_0 -$ monsoon thickness of shafts, $t_0 -$ the initial thickness of the flat material. If we derive the expression from (6), it is equal to the following.

$$\dot{x}_2 = -(R + r + h_0 + t_0)\dot{\varphi}\sin\varphi,$$
$$\dot{y}_2 = (R + r + h_0 + t_0)\dot{\varphi}\cos\varphi. \tag{7}$$

The base plate on which the flat material is suspended moves vertically and its potential energy is as follows.

$$\Pi = m_1 g(y_1 + y_2) = m_1 g((R + r + h_0)\sin\psi + (R + r + h_0 + t_0)\sin\varphi) \tag{8}$$

To formulate the differential equation of motion of a pair of elastically coated shafts, we consider that the process under consideration is under the influence of potential forces, and we use Lagrange's second-order equation of motion defined for a mechanical system under potential forces:

$$\frac{d}{dt}\frac{\partial L}{\partial \dot{q}_i} - \frac{\partial L}{\partial q_i} = 0 \quad i = 1...6 \tag{9}$$

That is, we have the following six equations.

$$\frac{d}{dt}\frac{\partial L}{\partial \dot{x}_1} - \frac{\partial L}{\partial x_1} = 0, \tag{10}$$

$$\frac{d}{dt}\frac{\partial L}{\partial \dot{y}_1} - \frac{\partial L}{\partial y_1} = 0, \tag{11}$$

$$\frac{d}{dt}\frac{\partial L}{\partial \dot{x}_2} - \frac{\partial L}{\partial x_2} = 0, \tag{12}$$

$$\frac{d}{dt}\frac{\partial L}{\partial \dot{y}_2} - \frac{\partial L}{\partial y_2} = 0, \tag{13}$$

$$\frac{d}{dt}\frac{\partial L}{\partial \dot{\psi}} - \frac{\partial L}{\partial \psi} = 0, \tag{14}$$

$$\frac{d}{dt}\frac{\partial L}{\partial \dot{\varphi}} - \frac{\partial L}{\partial \varphi} = 0. \tag{15}$$

In this $L = T - \Pi$ given. $L-$function of Lagrange, $T-$total kinetic energy, $\Pi-$potential energy.

Now we calculate the total kinetic energy. To do this, we can write the total kinetic energy in the following form, taking into account the sum of expressions (1) and (2) and expression (4):

$$T = T_1 + T_2 + T_3 + T_4 + T_5 = \frac{1}{2}m_1(\dot{y}_1^2 + \dot{y}_2^2) + 2\left(\frac{1}{2}m_2\dot{x}_1^2 + \frac{1}{2}J_{Cz}\omega^2\right) + 2\left(I_z\frac{\omega^2}{2}\right) = \frac{1}{2}m_1(\dot{y}_1^2 + \dot{y}_2^2) + m_2\dot{x}_1^2 +$$
$$+ J_{Cz}\omega^2 + I_z\omega^2 = \frac{1}{2}m_1(\dot{y}_1^2 + \dot{y}_2^2) + m_2\dot{x}_1^2 + \frac{m_2R^2}{2}\dot{\psi}^2 + \frac{3m_4R^2}{2}\dot{\varphi}^2$$
$$. \tag{16}$$

Determine Lagranges' function.

$$L = T - \Pi = \frac{1}{2}m_1(\dot{y}_1^2 + \dot{y}_2^2) + m_2\dot{x}_1^2 + \frac{m_2R^2}{2}\dot{\psi}^2 + \frac{3m_4R^2}{2}\dot{\varphi}^2 - m_1g((R + r + h_0)\sin\psi + (R + r + h_0 + t_0)\sin\varphi) \tag{17}$$

We now calculate the complete and specific derivatives of the Lagrange's function.

$$\frac{\partial L}{\partial \dot{x}_1} = 2m_2\dot{x}_1, \qquad \frac{d}{dt}\frac{\partial L}{\partial \dot{x}_1} = 2m_2\ddot{x}_1, \qquad \frac{\partial L}{\partial x_1} = 0. \tag{18}$$

$$\frac{\partial L}{\partial \dot{y}_1} = m_1 \dot{y}_1, \qquad \frac{d}{dt}\frac{\partial L}{\partial \dot{y}_1} = m_1 \ddot{y}_1, \qquad \frac{\partial L}{\partial y_1} = 0. \tag{19}$$

$$\frac{d}{dt}\frac{\partial L}{\partial \dot{x}_2} = 0, \qquad \frac{\partial L}{\partial x_2} = 0. \tag{20}$$

$$\frac{\partial L}{\partial \dot{y}_2} = m_1 \dot{y}_{2,} \qquad \frac{d}{dt}\frac{\partial L}{\partial \dot{y}_2} = m_1 \ddot{y}_2, \qquad \frac{\partial L}{\partial y_2} = 0. \tag{21}$$

$$\frac{\partial L}{\partial \dot{\psi}} = m_2 R^2 \dot{\psi}, \qquad \frac{d}{dt}\frac{\partial L}{\partial \dot{\psi}} = m_2 R^2 \ddot{\psi}, \qquad \frac{\partial L}{\partial \psi} = -m_1 g (R + r + h_0)\cos\psi. \tag{22}$$

$$\frac{\partial L}{\partial \dot{\varphi}} = 3m_4 R^2 \dot{\varphi}, \qquad \frac{d}{dt}\frac{\partial L}{\partial \dot{\varphi}} = 3m_4 R^2 \ddot{\varphi}, \qquad \frac{\partial L}{\partial \varphi} = -m_1 g (R + r + h_0 + t_0)\cos\varphi. \tag{23}$$

By substituting the complete and specific derivatives of the calculated Lagrangian function (18) - (23) into equations (10) - (15), we obtain the differential equations of motion of the working elastic shaft pairs.

$$2m_2 \ddot{x}_1 = 0, \tag{24}$$

$$m_1 \ddot{y}_1 = 0, \tag{25}$$

$$m_1 \ddot{y}_2 = 0, \tag{26}$$

$$m_2 R^2 \ddot{\psi} + m_1 g (R + r + h_0)\cos\psi = 0, \tag{27}$$

$$3m_4 R^2 \ddot{\varphi} + m_1 g (R + r + h_0 + t_0)\cos\varphi = 0. \tag{28}$$

In the research process, we need to ensure that the base plate moves at a constant speed, for which we obtain an integrated solution of the differential equations (24) - (25).

$$\dot{x}_1 = const,$$

$$\dot{y}_1 = const,$$

$$\dot{y}_2 = const \tag{29}$$

Given that the base plate moves at a constant speed, then the angular velocity of the shafts are equal to $\omega = \dot{\psi} = const$ and $\omega = \dot{\varphi} = const$ and angular acceleration is equal to $\varepsilon = 0$. In this case, the equations of motion (27) - (28) look like this:

$$m_1 g (R + r + h_0)\cos\psi = 0, \tag{30}$$

$$m_1 g (R + r + h_0 + t_0)\cos\varphi = 0. \tag{31}$$

We determine the coverage angle from equations (30) and (31).

$$\cos\psi = 0$$

$$\psi = \frac{\pi}{2} + \pi n, n \ni Z \tag{32}$$

$$\cos\varphi = 0$$

$$\varphi = \frac{\pi}{2} + \pi n, n \ni Z \tag{33}$$

Conclusion. Based on the above results, our research work includes: if we conclude that the base plate on which the flat material is laid leaves the coverage area of the shaft pairs covered with the first working elastic material and the shaft pairs covered with the second working elastic material hit the coverage area, from the solutions of the differential equations given in this case, it can be seen that the base plate moves along the chain at a constant speed. Also, based on equations (32) and (33) solved with respect to the coverage angle, we can say that the coverage angle must be less than 90° for the problem we are considering. If the coverage angle accepts values greater than 90°, we cannot achieve the expected result. Thus, even when the system we are looking at is under potential forces, the base plate is moving at a constant speed.

References.

1. Amanov, Auezhan T., Bahadirov, Gayrat A., Tsoy, Gerasim N., Nabiev, Ayder M, "A New Method to Wring Water-Saturated Fibrous Materials," Int. J. Mech. Eng. Robot. Res., vol. 10, no. 3, pp. 151–156, 2021, doi: 10.18178/ijmerr.10.3.151-156.
2. M. N. Zakharov and M. S. Kuts, "The approach to determine the elastic characteristic of the contact of rough surfaces," Int. J. Mech. Eng. Robot. Res., 2020, doi: 10.18178/ijmerr.9.7.937-942.
3. A. Djuraev and A. Jumaev, "Providing the development of new designs for the design of the roller mechanism transmitting rotational motion in belt conveyors," Int. J. Emerg. Trends Eng. Res., 2020, doi: 10.30534/ijeter/2020/267892020.
4. J. Liu, "A dynamic modelling method of a rotor-roller bearing-housing system with a localized fault including the additional excitation zone," J. Sound Vib., 2020, doi: 10.1016/j.jsv.2019.115144.
5. J. Liu, L. Luo, Y. Hu, F. Wang, X. Zheng, and K. Tang, "Kinetics and mechanism of thermal degradation of vegetable-tanned leather fiber," J. Leather Sci. Eng., 2019, doi: 10.1186/s42825-019-0010-z.
6. G. Bahadirov, G. Tsoy, and A. Nabiev, "STUDY OF THE EFFICIENCY OF SQUEEZING MOISTURE-SATURATED PRODUCTS," EUREKA Phys. Eng., 2021, doi: 10.21303/2461-4262.2021.001606.
7. G. A. Bahadirov, T. Z. Sultanov, and A. Abdukarimov, "Kinematic analysis of tooth-lever differential transmission mechanisms," 2020, doi: 10.1088/1755-1315/614/1/012101.

AGRICULTURAL ENGINEERING SOLUTIONS

ISSN: 2181-399X Volume 3, Issue 3, 2023

AGRICULTURAL ENGINEERING SOLUTIONS

AGGREGATE FOR INSTALLING THE DRIP TAPE IN A POTATO COMB

N. Martinova[1], K. Shavazov[2], N. Telovov[1], S. Toigambayev[1], A. Korneev[1]

[1]Russian State Agricultural University - MSHA named after K.A. Timiryazev, 127550, Russian Federation, Moscow,

[2]"Tashkent Institute of Irrigation and Agricultural Mechanization Engineers" National Research University, 39, Street Kari Niyaziy, Tashkent, 100000, Uzbekistan

Annotation. In this scientific article it is described that the substantiation the need for additional when growing potatoes in the Moscow region to obtain sustainable yields, indicates the unevenness of precipitation in the spring - summer period. The advantages of drip irrigation in comparison with other types of irrigation are given. One of the limiting factors for the widespread use of drip irrigation is the low degree of mechanization during the installation of drip tape. It has been proven that the combination of agro-technical operations will reduce energy consumption and increase work productivity. The water consumption of potatoes in different phases of plant life has been analyzed. The conditions for creating optimal water - air balance of the soil are considered. It is proved that in the initial period of plant development, the need for water is minimal, and the soil during this period, as a rule, is saturated with moisture formed during the process of snow melting. Therefore, it is rational to combine the installation of the drip tape with the operation to form ridges. The design of special equipment for laying the drip tape into the soil has been developed and the technical characteristics of the developed machine are given, the operating speeds and productivity of the machine is determined. The numerical values of the resistance of the drip tape laying have been determined and it has been proved that the installation of the working equipment on the ridge former will not lead to a noticeable increase in the traction resistance. It is recommended a drip tape settings for potato comb. The design of a drip irrigation system for growing potatoes is proposed, a list of the necessary working equipment is given. The water regime of the plant was determined at different stages of development and the irrigation rate and the time intervals between irrigations were corrected.

Key words: root zone, water consumption, irrigation rate, drip tape, drip flow rate, pulling resistance.

Introduction. The climate of the Moscow region is characterized by uneven precipitation. High-water years can be alternated with low-water years. Precipitation in summer is often stormy in nature, when a significant part of the moisture does not have time to be absorbed into the soil, but forms a surface runoff and goes into the water intake. Therefore, to obtain a sustainable harvest when growing potatoes, additional watering is required. [1, 2, 3]. The advantages of drip irrigation are the delivery of irrigation water directly to the root layer, which leads to significant savings in irrigation water and electricity and slows down the growth of weeds in the aisles, since they are much less moistened. Currently, the area of land using drip irrigation does not exceed 40 thousand hectares, which is less than 10 % of the total area of irrigated land in the Russian Federation. [4, 5]. This figure is significantly lower than in the USA, Israel and a number of European countries. The rate of introduction of drip irrigation into domestic agricultural machinery is significantly behind the indicators of the countries of Southeast Asia [6, 7]. One of the limiting factors for the introduction of drip irrigation into the agriculture of the Russian Federation is the low degree of mechanization when laying drip tape. In the United States, a number of companies produce specialized machines for placing drip tape to a depth of 45 cm, for example Andros, Rain Flo, Kenco Manufacturing, but there are no machines for placing drip tape in a potato comb in the line of these manufacturers. [8, 9, 10]. Since the potato ridge has a small width at the top of 14 - 16 cm and a height of 25 - 30 cm, for better fixation, the drip tape should be placed in the upper soil layer. The creation of a specialized machine for placing a drip tape in a potato ridge will increase the degree of mechanization when growing potatoes using drip irrigation, reduce labor costs and increase work productivity.

Materials and methods. While growing season, the need for water in potatoes changes. In the initial phase, the plant has sufficient reserves of moisture and nutrients from the mother tuber. During this period, the soil is saturated with moisture absorbed in the process of snow melting, so there is no need for additional irrigation. In the future, the need for water increases, reaching maximum values during the flowering period and the end of the growth of the tops. It is during this period that there may be a deficit of precipitation, or their uneven fallout. For normal plant development, the pore volume must be 65 – 80 % filled with water, a decrease in these indicators will lead to a slowdown in photosynthesis, and, consequently, to a decrease in yield. During this period, it is necessary to carry out additional watering. In the future, the water consumption of potatoes decreases slightly, but the need for additional irrigation remains until the period of wilting of the tops. It is rational to combine the process of laying the drip tape with the operation to form ridges, which is carried out 10-14 days after planting. For this, the working equipment for laying the drip tape should be placed on the comb former. In the process of research, it is necessary to determine additional traction resistance from laying a drip tape in the soil.

The resistance force of laying the drip tape consists of the resistance force of pulling the tape, which, in turn, consists of the friction of the tape in the stacker, overcoming the imbalance of the coil and its friction against the axis, as well as the resistance of the soil to the development:

$$F_{po} = R_{ng} + F_{lv} = R_{ng} + F_{lvr} + F_{ldr} + F_{ltr} =$$
$$= \mu \cdot G_p + k_p \cdot h \cdot b + \varepsilon \cdot h \cdot b \cdot v^2 +$$
$$+\left(f_o \cdot G_l \cdot d_o \cdot d_p^{-1} + 2 \cdot G_l \cdot l_e \cdot d_p^{-1}\right) \cdot \left(1 + \mathrm{e}^{f_o \cdot \beta}\right), \qquad (1)$$

where F_{lv} is the resistance of pulling the tape, kN; F_{lvr} - friction resistance of the tape in the stacker, kN; F_{ldr} - effort to overcome the coil imbalance, kN; F_{ltr} - resistance to friction of the coil on the axis, kN; R_{ng} - soil resistance to development, kN; f_o - coefficient of friction of the axle in the supports; G_l - weight of the tape coil, kN; d_o - axis diameter, m; d_p is the diameter of the coil, m; l_e - displacement of the center of gravity of the bay from the axis of rotation, m; β - tape wrap angle; μ - coefficient of friction of the working body on the ground; G_p - stacker weight, kN; k_p — resistivity to cutting, kN/m^2; ε - coefficient taking into account the effect of cutting speed on the resistance to digging; h - development depth, m; b - development width, m. The drip tape stacker consists of a spool and a guide tube mounted on a special frame. The guide tube, with the help of which the drip tape is placed in the soil, is bent downwards, and the opener is welded to it in front, to reduce the development resistance when forming a gap in the soil for laying the drip tape. The tape reel is mounted on a horizontal axis rotating on a support in the bearing assembly. The position of the spool is fixed by the pressure discs. There is a braking device on the vertical frame of the frame, the tension roller of which stops the unwinding of the tape when the machine stops moving. When the machine is moving, the drip tape is unwound from the spool and is placed along the guide pipe into the upper soil layer to a depth of 2 - 4 cm.

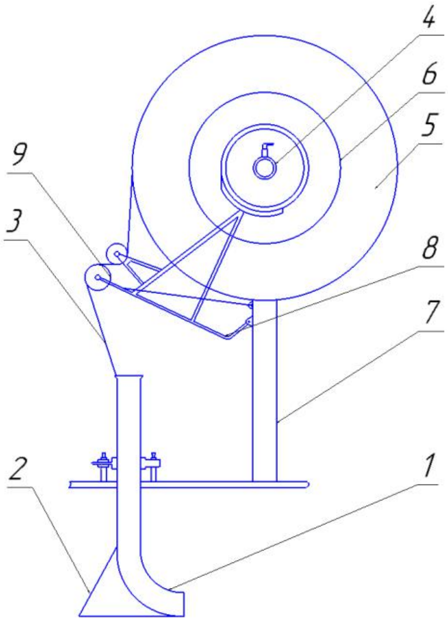

Figure 1. Construction of drip tape stacker:
1 - guide tube, 2 - opener, 3 - drip tape, 4- shaft, 5 - coil of drip tape, 6 - protective disc with latch, 7 - vertical support post, 8 - braking device, 9 - tensioning roller.

Based on the research results, an experimental model of the working equipment for laying drip tape into a potato comb was created. The model was tested in a dirt channel. During the tests, traction forces were measured (Figure 2).

Figure 2. Testing the drip tape stacker model in the soil channel.

The test results confirmed the data of theoretical studies, the resistance of the drip tape laying does not exceed 6 - 8% of the traction resistances arising during the formation of potato ridges. Therefore, it is possible to install additional working equipment on the ridge former for laying the drip tape into the potato ridge (Figure 3).

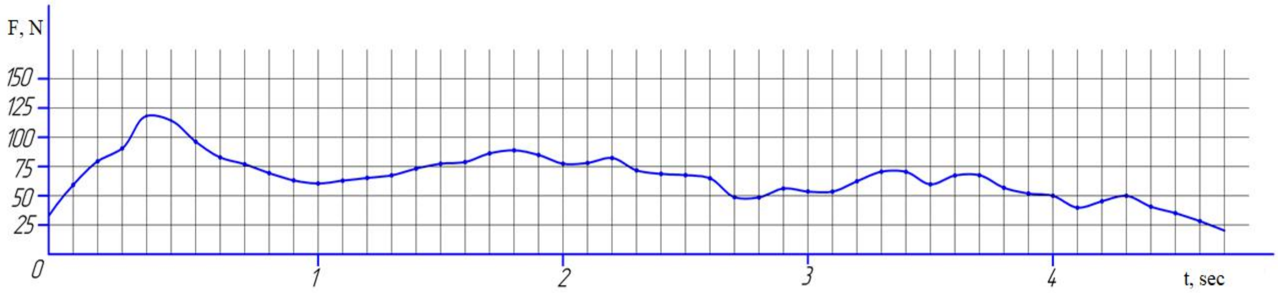

Figure 3. Drip Tape Laying Resistance Values.

Results and discussion. Based on the research results, the working equipment for laying the drip tape into the potato comb was manufactured and mounted on the Grimme GF-75/4 ridge former (Figure 4). The machine was tested at the Field Experimental Station of the K.A. Timiryazeva. In the process of testing, technological operations for laying a drip tape were worked out.

Figure 4. Laying drip tape while forming potato ridges.

Based on the potato planting scheme, for uniform moistening, a drip tape with a diameter of 16 mm was chosen with a flow rate of 1.6 l / h per drip chamber, with a distance of 30 cm between the emitters (Figure 5).

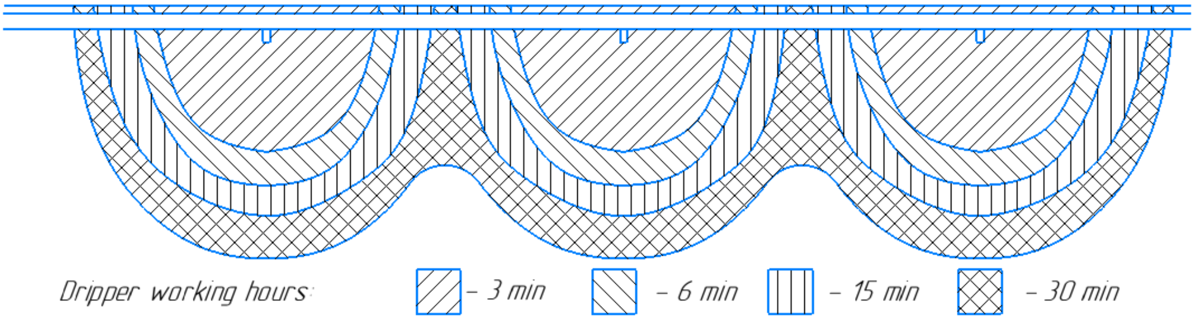

Figure 5. Formation of the humidification contour during the operation of the dropper.

During the tests, the working speeds were measured, the depth of the drip tape was monitored. The main parameters of the developed machine are presented in the table 1.

Table 1. Technical characteristics of the developed machine.

Working body weight	2150 kg
Working body width	3,0 m
Working speed	0,9 – 1,4 m/sec
Performance	0,51 – 0,97 ha/h
Drip tape diameter	16 mm
Dripper water consumption	1,6 L/h
Dripper spacing	300 mm

At the end of the installation of the drip tape, the drip irrigation system was installed (Figure 6).

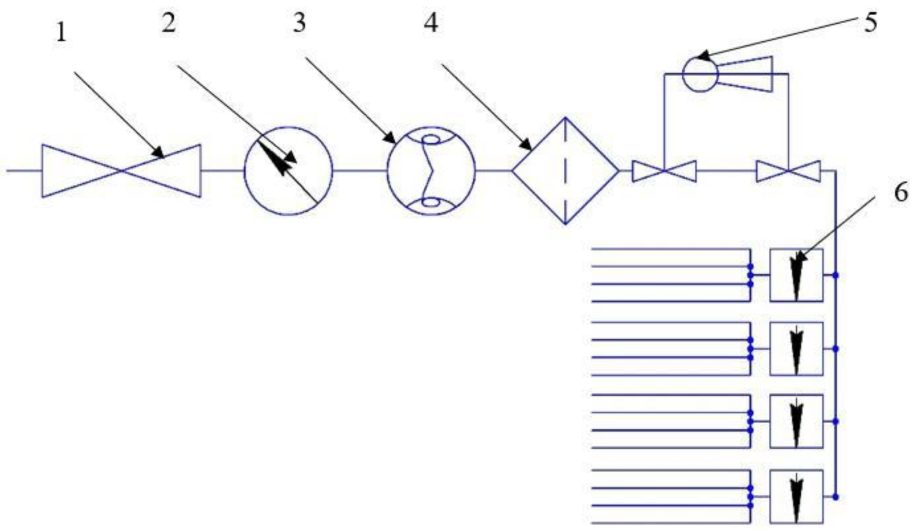

Figure 6. Drip irrigation system:
1 - tap; 2 - water pressure gauge; 3 - water meter; 4 - filter; 5 - dispenser; 6 - pressure regulator.

In the course of further research, the irrigation rate was adjusted for different phases of potato development. Watering was carried out before the wilting of the tops. Different areas were moistened alternately, watering was carried out at regular intervals (Figure 7).

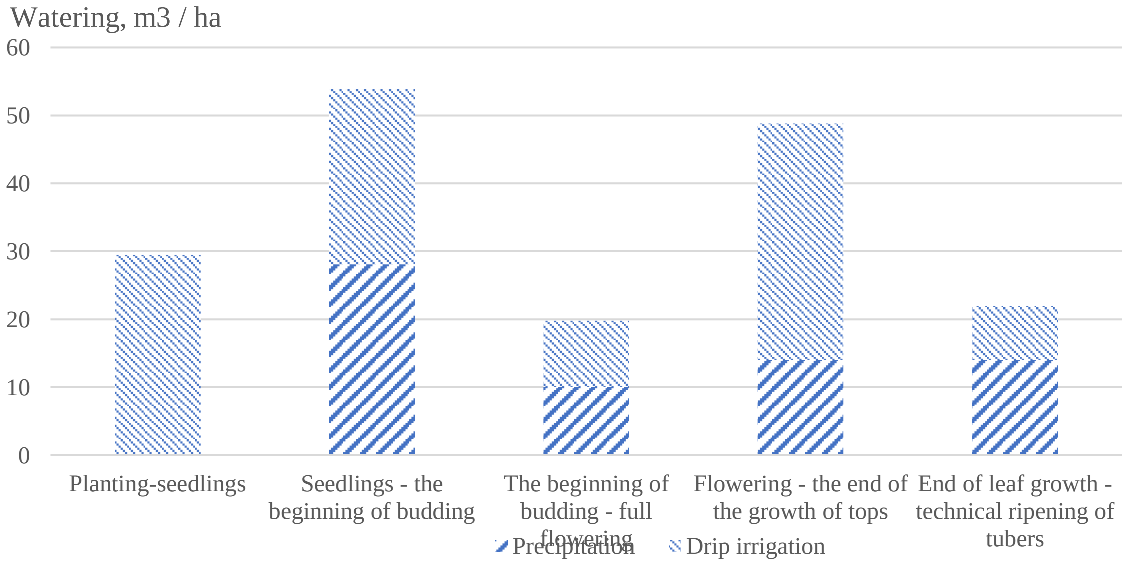

Figure 7. Water consumption of potatoes at different stages of development.

Findings. The climatic feature of the Moscow region is uneven precipitation in the spring and summer, therefore, to ensure a stable harvest, additional irrigation is necessary. The advantage of drip irrigation is the delivery of water directly to the root zone, which makes it possible to economically use irrigation water and inhibits the growth of weeds in the aisles. It is rational to lay the drip tape together with the operation to form potato ridges. Placing the equipment for laying the drip tape on the Grimme GF-75/4 ridge former did not lead to a noticeable increase in traction resistance. The use of a drip irrigation system made it possible to create an optimal water - air regime during the growing season of potatoes.

References.

1. Dubenok N.N., Bolotin D.A., Novikov A.A., Bolotin A.G. *Bulletin of the Nizhnevolzhsky agro-university complex: science and higher professional education* 2018 **51** (3) 81 – 90.
2. Starovojtova O.A., Shabanov N.E. *The Herald of the Moscow State Agricultural Engineering University named after V.P. Goryachkin* 2016 **74** (4) 34-40.
3. Reyes-Cabrera J., Zotarelli L., Dukes M.D., Rowland D.L., Sargent S.A. *Agricultural Water Management* 2016 **169** 183-192.
4. Martynova N.B., Korneev A.Yu. *The Herald of the Moscow State Agricultural Engineering University named after V.P. Goryachkin* 2018 **84** (2) 18 – 22.
5. Shtahko A.S., Shkura V.N. *Scientific journal of the Russian Research Institute of Melioration Problems* 2018 **31** (3) 39 – 57.
6. Vasiljev S.M., Shkura V.N., Shtahko A.S. *Bulletin of the Nizhnevolzhsky agro-university complex: science and higher professional education* 2018 **52** (4) 316 – 323.
7. Abdulmazhidov H.A., Matveyev A.S. *The Herald of the Moscow State Agricultural Engineering University named after V.P. Goryachkin* 2016 **72**(2) 40-46.
8. Ovchinnikov A.S., Buber A.A., Dobrachev Yu. P., Borodychev V.V. *Bulletin of the Nizhnevolzhsky agro-university complex: science and higher professional education* 2018 **54** (4) 65 – 76.
9. Ovchinnikov A.S., Bocharnikov V.S., Mesherjakov M.P., Bocharnikova O.V. *Bulletin of the Nizhnevolzhsky agro-university complex: science and higher professional education* 2017 **48** (4) 10 – 16.
10. Dubenok N.N., Bolotin D.A. Fomin S.D., Bolotin A.G. *Bulletin of the Nizhnevolzhsky agro-university complex: science and higher professional education* 2017 **48** (4) 22 – 29.

AGRICULTURAL ENGINEERING SOLUTIONS
ISSN: 2181-399X Volume 3, Issue 3, 2023

RESEARCHING THE PARAMETERS OF THE DISK ANGLE OF STEPPED TYPE PLOW

F. Mamatov[1], D. Chorieva[1*], N. Rashidov[1], B. Mukimov[2] and M. Hafullah[2]

[1]Karshi engineering-economics institute, 225, Mustakillik str., 180100, Karshi, Uzbekistan
[2]Karshi Institute of Irrigation and Agro technologies of the National Research University Tashkent Institute of Irrigation and Agricultural Mechanization Engineers, 180100, Karshi, Uzbekistan

Abstract. In this scientific article it is observed that the development and creation of energy-saving machines and technologies for high-quality basic processing is one of main tasks today. The existing step plows for smooth, row less plowing have a number of disadvantages. With these plows, the technology of smooth plowing is carried out in conditions of a closed furrow, as a result, they do not ensure the turnover of layers the required degree and the sealing of plant residues, and also have a high energy intensity. The purpose study is to substantiate the parameters the disk angle stepped plow. Theoretical studies were carried out using the methods of classical mechanics. Analytical expressions have been obtained to determine the permissible distance of transverse discarding of soil particles by a disk angle and the range of flight of soil particles under the action disk, depending on its parameters. Theoretical studies have established that the permissible distance of transverse discarding of soil particles by a disk angle should be no more than 29 cm. The analysis of the expressions obtained showed that with an increase in the diameter disk angle-lift, its angle of installation to the pressure of movement, the angle of inclination to the vertical of depth of processing the angle-lift, the range of transverse rejection of soil particles increases. To ensure the established distance of soil discarding, the diameter of the disk angle-lift should be no more than 480 mm, its installation angle to the direction the hole should not exceed 35°, the installation angle to the vertical should not exceed 10º and the processing depth should not exceed 11 cm.

Key words: stepped plow, spherical disc, body liner, disk diameter, angle installation

Introduction. The development and creation of energy-saving machines and technologies for high-quality basic processing is one the main tasks today. An integral requirement of a high culture of agriculture is the fundamental improvement technology of basic tillage through the development of new generation plows. Research on the development and application of non-egalitarian flat plow plows, on the justification of parameters their working parts Z. Uzakov [1], B. Tulaganov [2], F. Maiviatov [3-6], D. Irgashev [4], Yu. Syromyatnikov [7-9], A. Normirzaev [10], I. Ergashev [11], O. Sizov [12] and others. Three-body linear plug with a disc-shaped bevel is made and researched by F. Mamatov [1, 2] (Figure 1). In this plug, the disc-shaped burners the working surface upside down on the working surface the corals, which only sufficiently overturned the chambers chymed fields. In the research carried out, it was observed that in the process of working a linear plug, its working organs are clogged with soil and plug has been proposed by the O. Sizov consisting of bodies that are located upright in the direction of movement and the disc-shaped working organs that are installed in front of them. In the process of operation plug, the disc-shaped working organs in front bodies cut the corner plasts from the side furrow into the processing depth and throw it to the right over the plast and form an furrow in the form of a triangle close to its shape. The reliability workflow of the plug is extremely low and others proposed a plug to increase the reliability of turning the sledgehammers. A support is installed on the front edge of this plug, and in front housings, spherical disks are installed that cut the edge blade and turn it opposite to the tipping of blades, i.e. to the left. The literature does not provide information on tests of proposed plug A. Normirzayev [10] proposed to install a spherical disc in front rotary plow to ensure that it is not clogged with soil and plant residues and weeds are completely buried in the soil. F. Mamatov [1, 2] and I. Ergashev [11] proposed to install spherical disk-shaped reducers on the axis of symmetry opposing bodies, which are closed to the frame the frontal plug. However, in the mentioned studies, the issues mutual arrangement the working bodies and justification parameters spherical disk-shaped plow with an angle cutter, which implements flat plowing without an edge, have not been sufficiently studied.

The purpose study is to substantiate the parameters of disc angle of a stepped plow.

Materials and methods. According to the results research work carried out, it has been established that step plows for smooth, rowless plowing have a number of disadvantages. Due to the fact that these plows smooth plowing technology is carried out in conditions of a closed furrow, they do not provide the required degree of turnover of layers and the sealing of plant residues, and also have a high energy intensity. As a result, step plows do not carry out high-quality processing of fields, and their productivity is low. The analysis of research has shown that in order to ensure the required turnover of layers and the sealing of plant residues, as well as to reduce fuel consumption, labor and other costs during smooth, no-frills plowing, it can be achieved by using a step plow with disk angle-shifters.

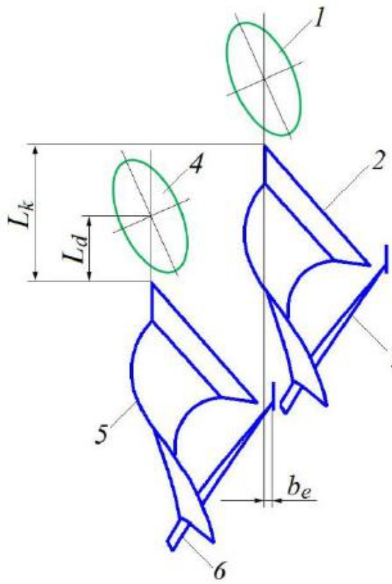

Fig. 1. Scheme of interposition of the sprocket plug disc shape angle controller and housing

During the operation disc-shaped angle cutter, the pieces of soil turned over by it should be located on the side plate. Otherwise, the soil particles blade rolled with the disk angle cutter will prevent the blade rolled with the front body from turning over at the edge of its edge, and the technological process may be disrupted. When the soil particles are thrown beyond the specified distance, they hit the front casing and fall to the bottom plow. The following condition must be met so that the soil particles overturned by the disc-shaped angle cutter do not touch the front body elements and the overturning plow and do not fall to the bottom plow.

$$L_t < b_p - b_d. \quad (1)$$

We determine the width b_d plate to be cut with a disc-shaped angle cutter according to the following expression

$$b_d = 2\sqrt{a_d(2R - a_d)}\sin\alpha\cos\gamma. \quad (2)$$

We put the value b_d in expression (1) according to expression (2)

$$L_t < 2\sqrt{a_d(2R - a_d)}\sin\alpha\cos\gamma - b_d. \quad (3)$$

(3) calculations based on the expression b_p=52.5 cm, $a_{dm}ax$=11 cm, R=24 cm, α=35º and g=10º. showed that it should not be larger than cm.

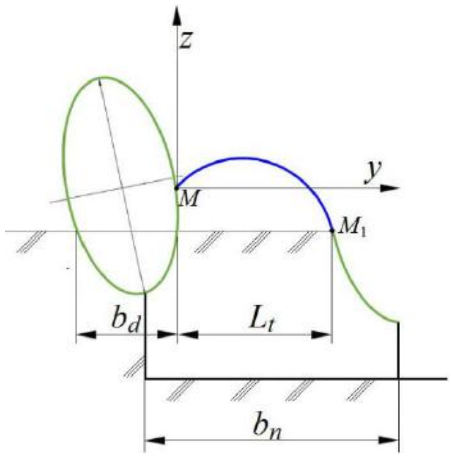

Fig.2. Schematic basis throw distance of overturned soil particles with a disk angle cutter

In order to determine the width soil turned over with a disc protractor, we will consider the process of turning over a log cut with it. In the process work, an angle cutter in the form of a spherical disc cuts and throws the earthen slab with an elliptical cross section to the side (Figure 2). In this case, we assume that the surface cross-section sawdust cut and turned over to the field surface is equal to each other, i.e.

$$F_1 + F_2 = S, \quad (4)$$

Based on Figure 3

$$F_1 = \frac{h^2 ctg\varphi_t}{2}; \qquad F_2 = \frac{h^2 ctg\varphi_k}{2}; \quad (5)$$

where φ_t – is the natural slope angle, degrees; φ_k – soil collapse angle, grad.

We put the values F_1 and F_2 according to (5) to (4)

$$S = \frac{h_u{}^2 ctg\varphi_t}{2} + \frac{h_u{}^2 ctg\varphi_k}{2}. \quad (6)$$

From expression (6)

$$l_1 tg\varphi_t = l_2 tg\varphi_k. \quad (7)$$

We determine the values l_1 and l_2 from the above expressions

$$l_1 = h_u ctg\varphi_t = ctg\varphi_t\sqrt{\frac{2S}{ctg\varphi_t + ctg\varphi_k}}, \quad (8)$$

$$l_2 = h_u ctg\varphi_k = ctg\varphi_k\sqrt{\frac{2S}{ctg\varphi_t + ctg\varphi_k}}. \quad (9)$$

In that case

$$L_u = l_1 + l_2. \tag{10}$$

We put the values l_1 and l_2 in (10)

$$L_u = ctg\varphi_t\sqrt{\frac{2S}{ctg\varphi_t + ctg\varphi_k}} + ctg\varphi_k\sqrt{\frac{2S}{ctg\varphi_t + ctg\varphi_k}}, \tag{11}$$

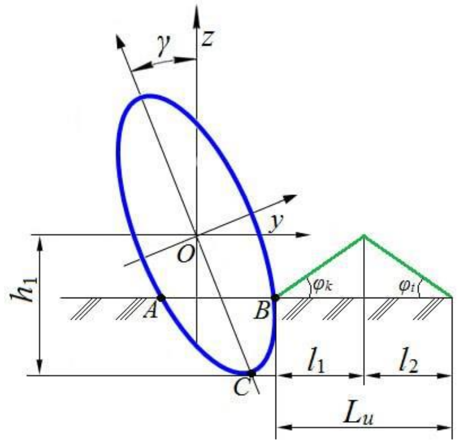

Fig.3. The scheme for determining the distance transverse throwing soil pieces with a disc-shaped protractor

Considering that $\varphi_1=\varphi_2=\varphi_k$

$$L_u = ctg\varphi_t\sqrt{\frac{2S}{ctg\varphi_t + ctg\varphi_t}} + ctg\varphi_t\sqrt{\frac{2S}{ctg\varphi_t + ctg\varphi_t}}. \tag{12}$$

M.Ergashev shows the face cross-section blade that can be cut with a disc-shaped angle cutter (11) can be determined by the following expression proposed by

$$S_1 = \frac{D\sin\alpha}{2h_1}\left[h_1^2\arccos\frac{h_1 - h}{h_1} - (h_1 - h)\sqrt{h_1^2 - (h_1 - h)^2}\right], \tag{13}$$

in this $h_1 = \sqrt{\frac{4cd}{4ac - b^2}}$ – the vertical distance from the bottom to the centers projections the disks lowered into the transverse-vertical plane, m;

$$c = \cos^2\gamma + \sin^2\gamma\cos^2\beta\sin^2\alpha;$$

$$d = 0{,}25D^2\cos^2\beta\sin^2\alpha;$$

$$a = \sin^2\gamma + \cos^2\gamma\cos^2\beta\sin^2\alpha;$$

$$b = \sin 2\gamma(1 - \cos^2\beta\cos^2\alpha);$$

$$\gamma = arctg\frac{tg\beta}{\cos\alpha}.$$

In this case, α is the depth of sinking the disk-shaped angle cutter into the soil.

We put the value of S in (12) according to (13).

$$L_u = ctg\varphi_t\sqrt{\frac{2\left\{\left(a_\partial - \frac{D}{2}\right)\sqrt{a_\partial(D - a_\partial)}\right) + \frac{D^2}{4}\left[\arcsin\left(\frac{2a_\partial}{D} - 1\right) + \frac{\pi}{2}\right]\right\}\sin\alpha}{ctg\varphi_k + ctg\varphi_t}} + \tag{14}$$

$$+ ctg\varphi_t\sqrt{\frac{2\left\{\left(a_\partial - \frac{D}{2}\right)\sqrt{a_\partial(D - a_\partial)}\right) + \frac{D^2}{4}\left[\arcsin\left(\frac{2a_\partial}{D} - 1\right) + \frac{\pi}{2}\right]\right\}\sin\alpha}{ctg\varphi_t + ctg\varphi_t}}.$$

Results and discussion. According to the expression (14), taking φ_t=40°, we determine the distance L_u cross throw a piece of soil with a spherical disc. The distance transverse throw lump of soil L_u is the depth of immersion angle cutter in the form of a spherical disc into the soil (a_d), the diameter spherical disc (D), the angle of its installation relative to the direction movement (α) and vertical (γ) graphs changes depending on are presented in Figure 4.

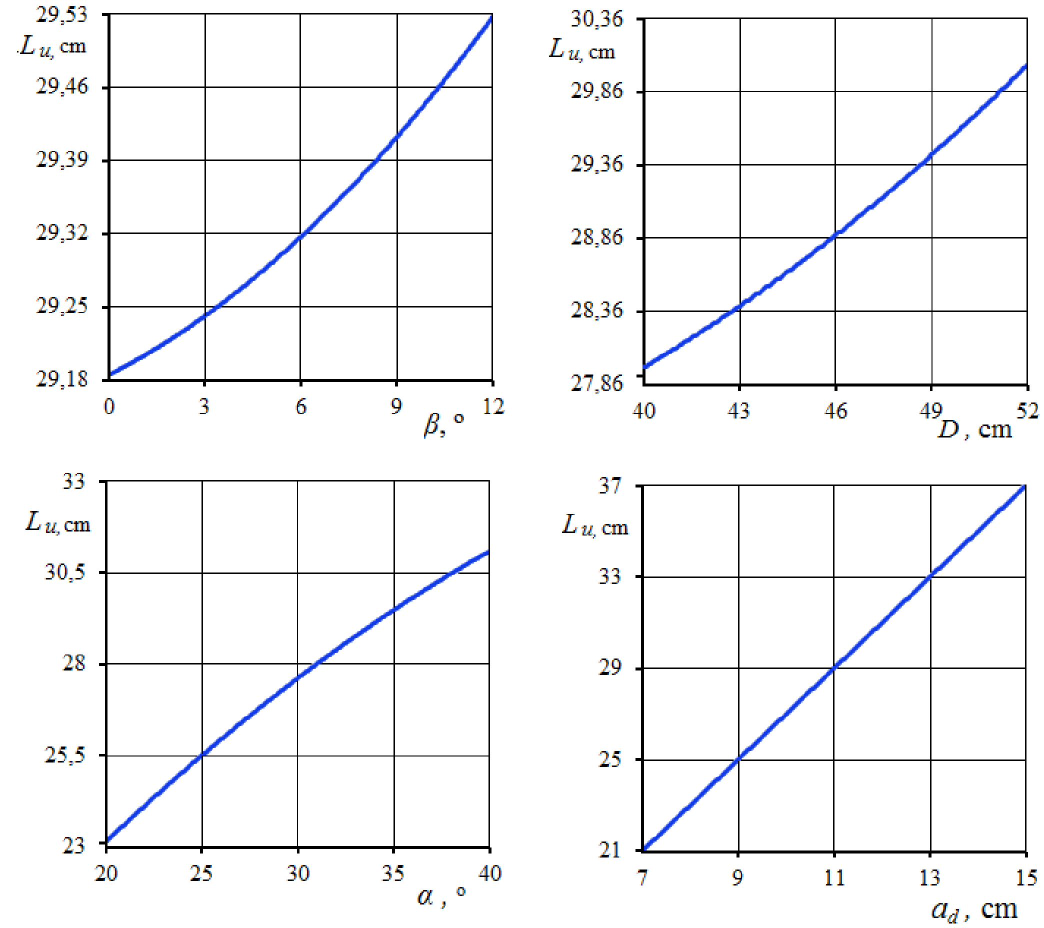

Fig.4. The distance transverse throw soil lump (L_u) depends on the diameter spherical disk (D) and its direction movement (a) and the angle installation relative to the vertical (b), the depth processing angle cutter (a_d) graphs of liq

As can be seen from the graphs presented in Figure 4, the distance crosswise throwing soil pieces increased with the increase disc angle cutter processing depth a_d, the direction of movement and the installation angles a and b relative to the vertical, as well as the diameter spherical disc D.

(14) calculations according to the expression and based on Figure 4, the diameter disc angle cutter is greater than 480 mm, its installation angle relative to the direction of movement is greater than 35°, the installation angle relative to the vertical is greater than 10º, and the processing depth is greater than 11 cm should not be.

Conclusions. Analytical expressions are obtained to determine the permissible distance of transverse ejection of soil particles by a disk angle and the flight range of soil particles under the influence disk depending on its parameters. Theoretical studies have established that the permissible distance for the transverse throwing of soil particles by a disk angle should be no more than 29 cm.

According to the results of theoretical studies, for cutting the slats to a specified distance with a spherical disk angle cutter, its diameter is 480 mm, the installation angle relative to the direction of movement is 35°, the installation angle relative to the vertical is 10º, and the depth of processing is it should not be more than 11 cm.

References.

1. Uzakov Z, Mamatov F, Begulov O 2019 International Conference on information Science and Communications Technologies 158120
2. Tulaganov B, Mirzaev B, Mamatov F, Yuldashev Sh, Rajabov N and Khudaykulov R 2021 IOP Conf. Series: Earth and Environmental Science 868 012062
3. Maiviatov F, Karshiev F, Gapparov Sh 2021 IOP Conf. Series: Earth and Environmental Science 868 012060
4. Irgashev D, Toshtemirov S, Maiviatov F, Muqimov B 2023 E3S Web of Conferences 390, 01036
5. Maiviatov F, Ravshanov K, Mamatov S, Temirov I, Kuvvatov D, Abdullayev A 2021 IOP Conf. Series: Earth and Environmental Science 868 01206
6. Maiviatov F, Karimov R, Musurmonov I, Choriev R, Saparov Sh 2023 E3S Web of Conferences 401,04028
7. Syromyatnikov Yu, Voinash S, Troyanovskaya I, Tikhonov E, Partko S and Sokolova V 2023 Journal of Terramechanics 108 1-5
8. Syromyatnikov Yu, Kuts A, Troyanovskaya I, Orekhovskaya A, Tikhonov E and Sokolova V 2022 Acta Technologica Agriculturae, 25 (2) 73-78
9. Syromyatnikov Yu, Orekhovskaya A, Klyosov D, Vodolazskaya N, Syromyatnikov P and Sementsov V 2022 Journal of Terramechanics 100 81-86
10. Normirzaev A 2017 Vestnik nauki i Tvorchestva № 1 (13) 86-90
11. Ergashev I, Maxmudov M, Islomov Yo 2005 Journal Problems of Desert-grazing Cattle Breeding Development 230-232

AGRICULTURAL ENGINEERING SOLUTIONS
ISSN: 2181-399X Volume 3, Issue 3, 2023

RESEARCHING THEORETICALLY AND PRACTICALLY OF THE PROCESS OF MOVING THE COTTON BY AIR TO THE PIPES OF THE CARRIER DEVICE

O. Sarimsakov[1], F. Kadirova[2]

[1]Namangan Engineering and Technology Institute,
[2]Namangan engineering-construction institute, Namangan, 160103, Uzbekistan
Olimjon5008@mail.ru; qodirovaferuza593@gmail.com

Abstract. In this article, results of the theoretical and practical are described. The comprehensively analyzes the scientific research on the transfer of cotton to an air-assisted carrier. Based on the results of theory and practical work, the theoretical basis of the process of transferring cotton to an air-assisted carrier device was created. When transmitting raw materials to the starting part of the pipe of the carrier device using air at different starting speeds, the movement trajectories of cotton in the distance to the pipe and inside the pipe were determined. In this case, it is theoretically proven that cotton moves in the initial part of the pipe and gradually moves into the rectilinear movement.

Key words: cotton, transfer, pipe, air, device, machine, horizontal tape, shaft, screw breaker

Introduction. Currently, at the beginning of the technological process of cotton ginning enterprises, the mechanized transmission of cotton by air to the pipe of the carrier device system is carried out using the RBX brand screw breaker machine. The work of RBX garam breaker machine was studied at Namangan cotton ginning plant. With the help of the RBX pile milling cutter, it breaks the pile and gives the cotton to a horizontal tape device. It in turn transmits air to the carrier device pipe. There are options for moving up and down the stream with a pile milling machine installed and sliding next to it. Such an opportunity will increase the efficiency of its demolition of cotton from garam. The process of transferring cotton from the garam breaker machine garam is carried out in two stages in the specified scheme. In the first, a screw breaker machine is able to move along the length of the shaft, distorting the part of it around 6 meters. In it, the distance between the horizontal tape device and the stair is 5 meters.[1, 5]

In the second stage, the boiler Breaker will be able to transmit the remaining 8 meters of the width of the cotton boiler. In this case, a horizontal tape device is installed on the cotton collection pad.

Methods and materials. Having studied the condition of the cotton being transferred with the heap eliminator, we came to the fo llowing conclusion. The milling machine with its pegs breaks the cotton from the pile and transmits it to the tape in the ball position, and the cotton is distributed unevenly over the tape. As a result, an uneven transfer of cotton to the pipe of the carrier device with the help of air occurs. In order to study this in detail, the experimental device scheme was developed and prepared at the Namangan cotton ginning enterprise No. 3 (Figure 1). This air-assisted carrier consists of a screw breaker with a curved tape device (1) and a horizontal tape device (2) and an air-assisted carrier (3). A horizontal tape device is mounted along the screw breaker positioning line [6].

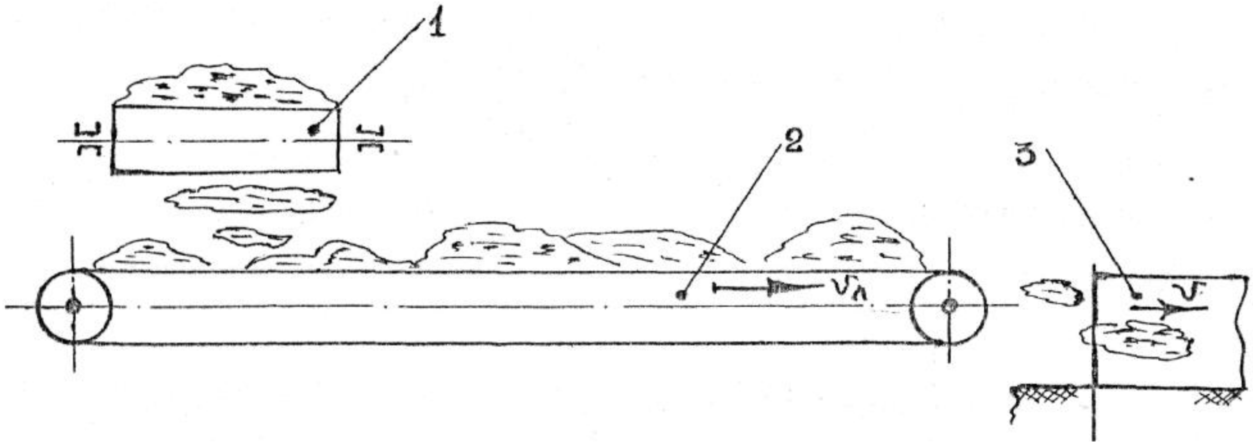

1 –bias tape devise ; 2-horizontal tape devise; 3-a tube which carries the cotton

Figure 1. Scheme of an experimental device prepared for the study of unevenness in the transmission of cotton

The method of conducting the study is as follows: the equipment prepared for the study was conditionally divided into 10 equal sections of the length of the horizontal transporter, which is installed parallel to the fault-breaking alignment line. The linear speed of movement, the width and length of the tape, the dimensions of the plots were determined, scales were prepared for pulling cotton [7].

Research results. The output side of the transporter is designed to transmit material directly to the pipe. The air-assisted carrier device separator and fan, horizontal transporter and throttle Breaker was installed according to the current operating rules. During the study, the operation of the screed breaker and separator is regularly monitored, special attention is paid to the process of transferring cotton. After 60 Minutes, the screw breaker and horizontal tape device was stopped at the same time. In this, a spread of cotton is formed on the surface along the length of the tape. It characterizes the state in which the material from which the spread is transmitted is transmitted.

On the surface of the resulting spread horizontal tape cut into pieces according to the specified plots.

Each piece weighed and the weight of the Cotton was determined for each piece separately and without generalization.

Experiment is repeated 3 times.

The unevenness indicator was developed according to a special methodology:

$$S = \sqrt{\frac{\sum_{l=1}^{n}(k_i - k_{cp})}{n-1}} \tag{1}$$

Here: *S*- dispersion of material specific density along the surface of the tape; $k = \frac{m}{F_л}$ - criterion characterizing the magnitude of the weight of the material corresponding to the belonging area; *m*-the weight of cotton on the given plot of the tape; $F_л$ - area of the tape plot being seen; *n*-number of plot *(n=10).*

The transmission productivity of the device is found by the following formula, depending on the mass of cotton on the tape:

$$П = 3{,}6\frac{m \cdot V_л}{L} \qquad m/c \qquad (2)$$

Here: *m*- the mass of cotton on the tape,kg; *V tape speed*, м/c; *L* –tape length m.

1-Table. Results of research on the unevenness of the transmission of cotton by air to the carrier device

Demonstrators					
Cotton sort and variety	Humidity%	Bulk density kg/m^3	Productivity t/hour	Comparative density dispersion kg/m^2	Breakdowns over 1 hour
C6524	9,5	66,6	9,7	1,61	1^г
II type	9,5	75,6	9,5	2,33	1^г
hand picking	9,5	83,4	9,97	2,74	2^г, 1^с
C6524	11,2	69,2	9,2	2,11	2^г
II type	11,2	74,4	9,1	2,62	1^г
car picking	11,2	89,7	9,8	3,06	4^г, 2^с

As can be seen from Table 1, when transferring cotton, its unevenness will be high. This indicator increases depending on the increase in the volumetric density of the cotton and the high humidity. This situation occurs as a result of excessive compaction of cotton from garam. The screw breaker machine cannot vibrate the Cotton at the required level. Observations have shown that in high unevenness, cotton settles on the surface of the tape as pistols, with a large density and weight, and hides a certain cross-section of the input when entering the pipe. If, in this way, the pieces enter the pipe, a large aerodynamic shadow will be characteristic behind it during the transportation process. In this zone, the air pressure is significantly lower, after which the piece falling into the pipe falls to the bottom of the pipe, not getting the necessary aerodynamic force. Here, the line of aerodynamic forces is also joined by the resistance force generated by the penetration of cotton into the inner surface of the pipe, and the pipe Inlet is clamped.

During the study, the clogging of cotton in the pipe at low humidity and not too large volumetric density for an hour was observed 2 times at the entrance, once in the separator chamber. And in the case of large humidity and volumetric density, 4 times there was a blockage at the entrance to the pipe, 2 times in the separator chamber.

The negative effect of blockages in the Separator chamber will be especially great. To eliminate blockages in the separator, an average of 25 minutes of production time is spent, depending on its severe-lightness level. A break in the separator cider vinegar can also occur in this, and it will take extra time to replace it. In addition, when the separator's chamber is clogged with Cotton, Cotton will overflow into the working Chamber of the stoneware. This is overlooked during production. As a result of this, only part of the cotton is absorbed by the air. The rest of the way ends up in the rock-collecting bunker of the quarry.

From the above, it can be concluded that it is necessary to reduce the unevenness in the transmission of cotton. This provides an opportunity to increase the performance of all elements of the air-assisted carrier and the equipment that forms the technological chain of cotton processing.

It is necessary to develop a theoretical framework for conducting research on an air-assisted carrier device. Through this, it is required to carry out a more accurate study, which fully reveals the process of collision of cotton with all working organs of the carrier device using air. And on the basis of this, it is possible to improve the structures of the device elements.

Theoretical verification of the process of transferring cotton to the pipe. The air-assisted transport process represents the flow of air particles moving inside the pipe using the air pressure generated by the fan inside the device, and of solid bodies and particles moving by means of aerodynamic resistance to them and frictional forces. When transporting cotton by air, the concentration of air and cotton mixture has a significant effect on the nature of Transportation.

Resistance forces with inertial forces practically do not change in size at the time when the Material moves in a straight line pipe using air. In this case, the transmission of cotton along the axis of the pipeline of the carrier device using air creates favorable conditions for the transportation process.

The absence of theoretical developments in the selection of favorable conditions when transferring cotton to the pipe puts the issue of studying from the theoretical side the process of transferring cotton to the pipe of the carrier device using air. The solution of this issue ensures the moderate course of the air-assisted transportation process.

Transfer cotton to the pipe and study its movement inside. Let the tape device be used when transferring cotton to the pipe of the carrier device using air figure 2.

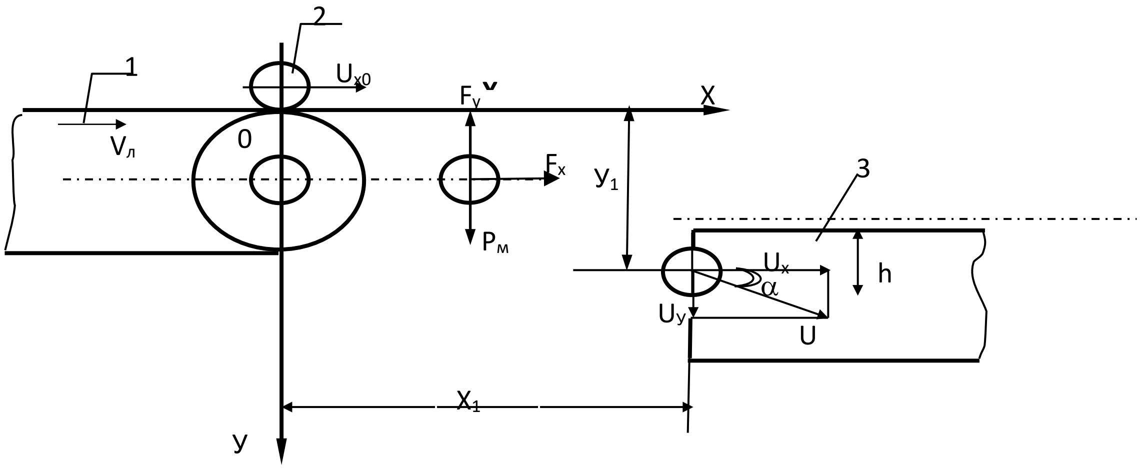

Figure 2. Transmission of cotton to the pipe of the carrier device using air using a tape device. 1-horizontal tape device; 2-piece of cotton; 3-pipe

Let's look at the movement of a piece of cotton on the HOU plane. First, we put the coordinate at the point where the contact of the tape with a cotton swab is interrupted.

The slice cut from the tape is affected by aerodynamic and weight forces. The equation of motion will look like this:

$$\begin{cases} m\dfrac{dU_x}{dt} = -F_x \\ m\dfrac{dU_y}{dt} = -F_y + P_м \end{cases} \qquad (3)$$

Here: m mass of piece, kg; U_x, U_y- the velocity of the slice on the coordinate axes is.

$$F_x = k_n U_x; \quad F_y = k_n U_y, \qquad (4)$$

In this: F_x, F_y - aerodynamic forces against the movement of the particle on coordinate axes; $P_м = mg$ - weight force; g - free fall acceleration; k_n - aerodynamic resistance coefficient of a piece of cotton.

Putting the equation of the acting forces and developing the system, we get:

$$\frac{dU_x}{dt} = -\frac{k_n}{m}U_x$$
$$\frac{dU_y}{dt} = -\frac{k_n}{m}\left(U_y - \frac{mg}{k_n}\right) \quad (5)$$

(2.5) solutions to the equation x, y - gives the velocities of a piece of cotton on coordinate axes. By integrating the solutions once in time, one obtains $y(t)$ and $x(t)$ - time from solutions subtracting the results of t $y = y(x)$ - we take the law of change of the movement of a piece of cotton:

$$y = -\frac{m^2 g}{k_n^2}\cdot\left[\ln\left(1 - \frac{k_n \cdot x}{mU_{x_0}}\right) + \frac{k_n \cdot x}{mU_{x_0}}\right] \quad (6)$$

By this law, we separate the cotton from the surface of the tape and build a graph of the trajectory of movement up to the pipe (Figure 3).

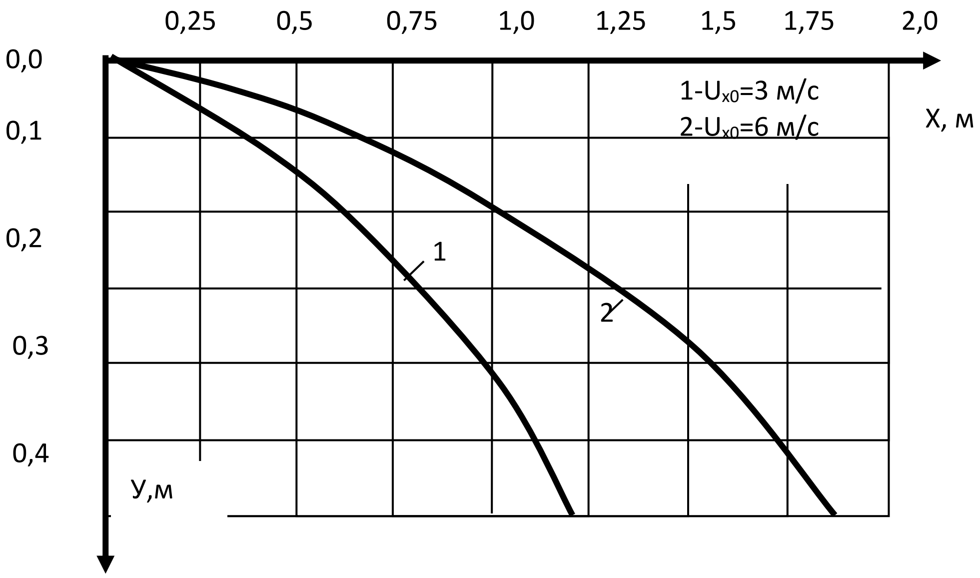

Figure 3. The trajectory of movement of cotton to the pipe.

Figure 3 depicts the trajectory of the movement of a piece of cotton prior to its arrival in the pipe of the carrier device using air.As can be seen from the graph, the piece moves along the ascending trajectory after separating from the surface of the tape, in which, at a small initial speed, the piece comes to the pipe with a small speed, at a large speed –on the contrary.

At the time of studying the movement of cotton in the pipe absorber, so that it is convenient, we first put the coordinate at the beginning of the pipe. Let's assume that the particle is moving between two infinite walls:

$y=0$ and $y=d.$

Let's assume that a piece of cotton during a meeting with an air flow has an absolute speed, moving it at a certain angle relative to the pipe axis. Then the equation of motion becomes:

$$\begin{cases} mx'' = -k(x' - V) \\ my'' = ky' - mg \end{cases} \tag{7}$$

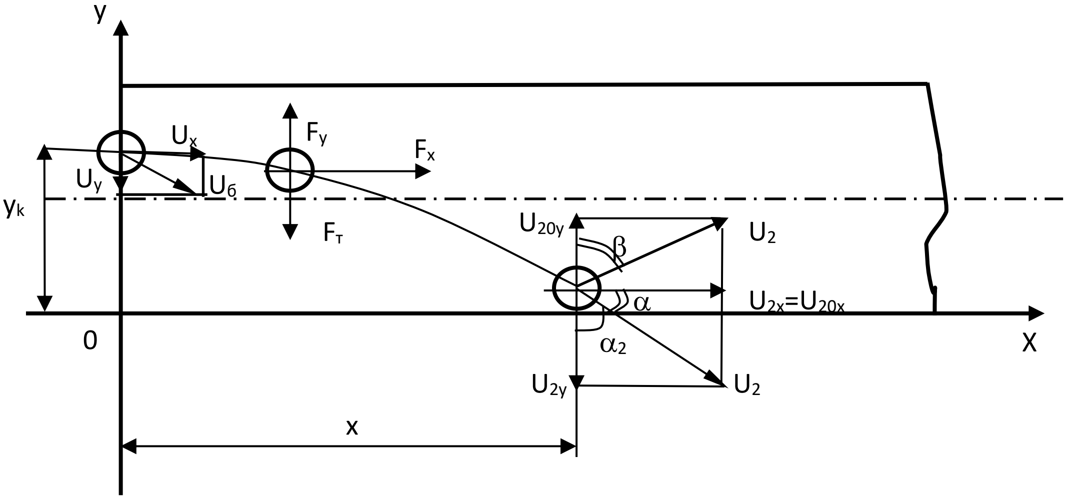

Figure 4. Movement of cotton in the pipe

$U_x = \dfrac{dx}{dt}$ and considering the $U_y = \dfrac{dy}{dt}$, (7) we integral the system under condition t = 0. The solution would be:

$$\begin{cases} x = \dfrac{m}{k}(U_H \cos\alpha - U)(1 - e^{-\frac{k}{m}}) + Vt \\ y = -\dfrac{m}{k}(U_H \sin\alpha - \dfrac{mg}{k})(1 - e^{\frac{k}{m}}) + \dfrac{mg}{k}t + y_1 \end{cases} \tag{8}$$

This system of equations determines the trajectory of the cotton to settle in the Hou plane.

At a certain distance (X), the piece collides with the inner wall of the pipe and is fired upwards under the influence of shock force.

From the scheme in Figure 4 we find the following equality:

$$tg\alpha = tg\left(\frac{\pi}{2} - \alpha_2\right) = ctg\alpha_2 \qquad \text{or} \qquad tg\beta = \frac{ctg\alpha_2}{n} \tag{9}$$

here: n - recovery coefficient.

Based on analytical calculations, the expression of the velocity of the post-impact cotton swab and the coordinate axes (x, y) let's determine the location on:

$$\begin{cases} U_x == (U_{20x} - V)l - \dfrac{k}{m}(t - t_1) + V \\ U_y = \left(U_{20y} - \dfrac{mg}{k}\right) l \dfrac{k}{m}(t - t_1) + \dfrac{mg}{k} \end{cases} \tag{10}$$

$$\begin{cases} \mathrm{X} = \dfrac{m}{k}(U_{20x} - V)\left(1 - l - \dfrac{k}{m}(t - t_2)\right) + V(t - t_2) \\ \mathrm{Y} = \dfrac{m}{k}\left(U_{20y} - \dfrac{mg}{k}\right)\left(1 - l\dfrac{k}{m}(t - t_2)\right) + \dfrac{mg}{k}(t - t_2) \end{cases} \tag{11}$$

here: $U_{20x} = (U_n \cos\alpha_1 - V)\dfrac{k}{m}t_2 + V \qquad U_{20y} = U_{20x}x \cdot tg\beta$

(10) and (11) the equations determine the position of the splitter at the first stroke on the pipe wall. In this, the slice reaches the critical point and goes down. If the vertical coordinate magnitude of the critical point is greater than the diameter of the pipe, then the piece will hit the upper wall. Its subsequent state can be determined with sufficient accuracy by equations of the Form (10) and (11). Only, modifications are made taking into account the direction of the initial speed after the stroke [16].

(11) time from expression subtracting the results of t

$y = y(t)$ - the law of change of the trajectory of a piece of cotton on the diameter and length of the pipe is graphically illustrated.

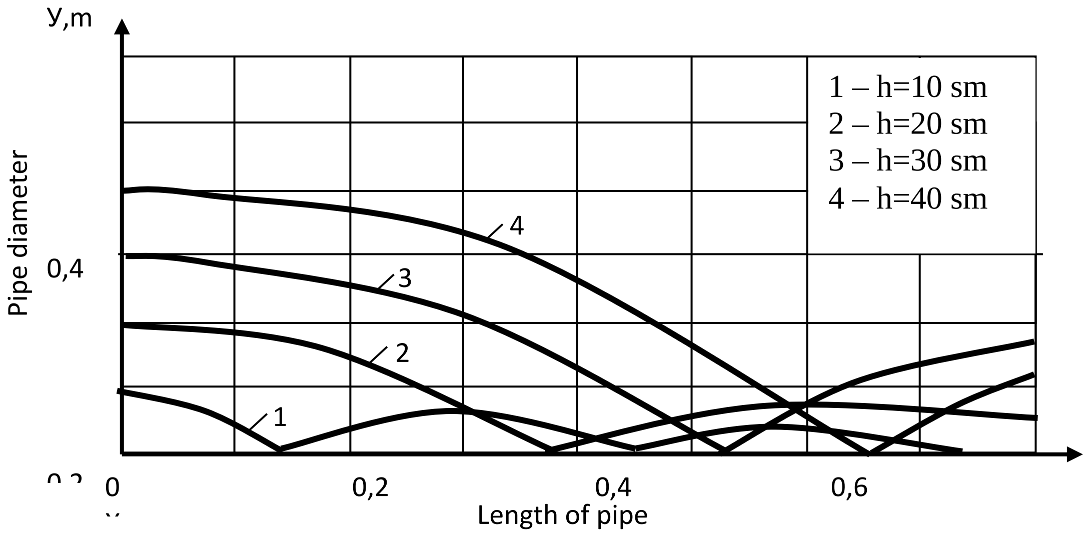

Figure 5. The trajectory of movement of a piece in a pipe.

An interesting case can be observed from the results, that is, during the movement of a piece of cotton in a pipe, a collision of a piece with a blow to the wall of the pipe occurs, even without taking into account the turbulence of the flow, longitudinal, rotating and other forces. The larger the velocities in this, the faster and more intense the shock.

Conclusions. Based on the results of theoretical and practical work with a comprehensive analysis of scientific research on the transmission of cotton to an air-assisted carrier, we draw the following conclusions:

The theoretical basis of the process of transferring cotton to an air-borne device was created.

When transmitting raw materials to the starting part of the carrier device pipe using air at different starting speeds, the movement trajectories of cotton in the distance to the pipe and inside the pipe were determined. In this, it was proved in a theoretical way that Cotton moves with jumps at the beginning of the pipe and gradually moves into a straight-line movement.

Based on the theory of movement of cotton at the beginning of the pipe, an equation was found for the effect of the speed of transmission of cotton on the pressure of the air consumed to accelerate it. The higher the initial speed it was found that the less energy consumption it would take to accelerate cotton.

References.

1. Arifjanov, A., Samiyev, L., Akhmedov, I., Atakulov, D. Innovative technologies in the assessment of accumulation and erosion processes in the channels (2021) Turkish Journal of Computer and Mathematics Education, 12 (4), pp. 110-114.DOI: 10.17762/turcomat.v12i4.481
2. Arifjanov, A., Akmalov, S., Akhmedov, I., Atakulov, D. Evaluation of deformation procedure in waterbed of rivers. (2019) IOP Conference Series: Earth and Environmental Science, 403 (1). DOI: 10.1088/1755-1315/403/1/012155
3. Arifjanov A., Atakulov D., Akhmedov I., and Hoshimov A.. Modern technologies in the study of processes in channels. In IOP Conference Series: Earth and Environmental Science, 1112(1), (2022)
4. Tadjiboyev S., Qurbonov X., Akhmedov I., Voxidova U., Babajanov F., Tursunova E., Xodjakulova D. Selection of Electric Motors Power for Lifting a Flat Survey in Hydraulic Structures. AIP Conference Proceedings 2432, (2022); https://doi.org/10.1063/5.0089643
5. Abduraimova D., Rakhmonov R., Akhmedov I., Xoshimov S., Eshmatova B. Efficiency of use of resource-saving technology in reducing irrigation erosion. AIP Conference Proceedings 2432, (2022) https://doi.org/10.1063/5.0089645
6. Arifjanov, A., Babajanov, F., Akhmedov, I., Fozilov, O., & Umarov, I. (2023). Analysis results of data obtained in natural field research in mountain river sokhsoy. Paper presented at the E3S Web of Conferences, , 365 doi:10.1051/e3sconf/202336503017
7. Arifjanov, A., Akhmedov, I., Umarov, I., & Kazadayev, A. (2023). Assessment of the influence of river sediments in the Sokhsoy river. In *E3S Web of Conferences*, https://doi.org/10.1051/e3sconf/202339004035

AGRICULTURAL ENGINEERING SOLUTIONS
ISSN: 2181-399X Volume 3, Issue 3, 2023

RESERCHING THE PARAMETERS OF THE FEED DISPENSER DISCHARGE WINDOW

K. Astanakulov[1], F. Mamatov[2], F. Karshiev[3]*, D. Khudaynazarov[4] and Sh. G'apparov[5]

[1]National Research University "Tashkent Institute of Irrigation and Agricultural Mechanization Engineers", 39, Street Kari Niyaziy, Tashkent, 100000, Uzbekistan
[2]Karshi engineering-economics institute, 225, Mustakillik str., 180100, Karshi, Uzbekistan
[3]Termez State University, 43, Barkamol avlod str., 190111, Termiz, Uzbekistan
[4]Tashkent State Technical University, university str. 2, Tashkent 100095, Uzbekistan
[5] Chirchiq Higher Tank Command and Engineering School, avenue Amir Temur, block of flats 1st, 15 , 111715, City: Chirchik, Uzbekistan

Abstract. In this scientific article, it is described that, currently, in world practice, feed spreaders are designed for large livestock farms, so they do not work well when used in family farms with 5-10 head of cattle or 50-60 head of sheep. The purpose of the study is to substantiate the parameters of the unloading window of a feed dispenser for family farms. A small device for distributing coarse feed has been developed for family farms. It consists of a hopper, a rotor, walking wheels, an electric motor, a worm gear, a belt drive and a discharge chute. Crushed straw, corn and alfalfa stalks were selected as roughages in the experiments. To determine the height and width of the spill window, one-factor experiments were conducted using the existing regulations on the developed device. According to the results of the conducted experiments, in order to ensure the quality of distribution of coarse feed at the level of the specified requirements, the width of the discharge window of the distribution device should be 40 cm. In this case, the amount of feed spillage is 4.71 kg/m in corn, 4.27 kg/m in alfalfa and 3.43 kg/m in straw and satisfies the initial requirements. The height of the pouring window should be 30 cm to ensure the required quality of pouring ground corn, alfalfa and straw. The amount of distributed mass is 3 kg to 5 kg per daily ration, 4.35 kg/m in corn, 4.05 kg/m in alfalfa, and 3.55 kg/m in straw, which is at the level of the specified requirements. According to the results of the experiment, the height of the discharge window of the developed distributor device was assumed to be 30 cm and the width was 40 cm.

Key words: feed dispenser, corn, chopper, substantiation, device, coarse, daily ration

Introduction. Currently, there are feed preparation and distribution devices designed for large livestock farms, while feed shredders have been developed for use on small livestock farms and private family farms. However, due to the lack of feed distribution equipment for small farms, this work is done by hand. This leads to low work quality and high labor costs [1-3].

The preparation of fodder for feeding livestock necessarily includes their grinding, mixing and distribution. These operations are mainly used to determine feed efficiency and animal productivity. Combining two or more operations in one technical tool is the most reasonable from an economic point of view, because it reduces the energy and metal consumption of the process of preparing complete feed mixtures, as well as the number of loading, unloading and transportation operations [4].

Livestock industry is one of the important sectors of agriculture of our country. Nowadays, there are many small farms specializing in livestock. Increasing productivity in livestock farming depends on good feeding of livestock with different types of fodder. The method of grazing livestock in the summer pastures of the desert or foothills leads to a significant reduction of the flora, as well as severe land degradation [5-7].

Today, several types of machinery and grinders are developed and used for the cultivation and harvesting of wheat, barley, soy, alfalfa, corn and fodder crops, as well as grinding of coarse and concentrated feed for these farms.

But for these small farms, this work is done by hand due to the lack of a spreader that mixes coarse and concentrated feed together. This causes increased labor costs, poor mixing of nutrients and uneven distribution [8-11].

In agricultural production, various structural and technological schemes are used for the preparation and distribution of feed in livestock farms. The most common technology for feeding young cattle on farms is the distribution of feed by mobile spreaders. The specificity of feed preparation and distribution processes for small cattle farms shows the need to develop specific solutions for the mechanization of feed distribution in these farms.

For this reason, it is urgent to develop a device that distributes crushed coarse fodder for livestock in small family livestock farms according to the daily ration in the same qualitative manner.

Considering the above, a small-sized, low-metal, low-energy, resource-saving feed dispenser for family livestock farms was developed, and the theoretical and experimental dimensions of the height and width of the discharge window were determined.

Materials and methods. GOST 34748-2021 "Agricultural machinery. Feed distributors. Test methods", GOST 20915-75 "Agricultural machinery. Methods for determining test conditions" "Feed mixtures". The methods given in the standard method manual "Technical conditions" were used [6-9].

Based on the above, a small device for distributing coarse feed was developed for family farms. The device consists of a hopper, a rotor with a shovel that pours feed, walking wheels, an electric motor, a worm gear, a belt drive and a pouring chute (Fig. 1).

1-wheels; 2-switch; 3- handle; 4- bunker; 5- pouring window; 6-rotating shovels; 7- drain; 8-drain window door; 9-electric motor; 10- reducer; 11- belt drive

Figure 1. Of the coarse feed distribution device trial copy

Chopped straw, corn and alfalfa stalks were selected as roughages, and the quality of their distribution largely depends on the height and width of the discharge window. Taking this into account, the dimensions of the height and width of the pouring window, which ensure the distribution of the amount of feed specified in the initial requirements and specifications of the device, were experimentally researched [9].

The experiments were carried out in a one-factor model, where the number of blades in the rotor is 2 pieces, and the number of rotations of the blade rotor is 50 r/min. First, in order to study the width of the pouring window in this part, experiments were conducted by changing the width of the pouring window from 30 cm to 45 cm with an interval of 5 cm.

The feed and distribution distance was determined to be 10 meters, and from this, the mass of the feed in the middle part of 5 meters was taken and it was found to be uniform in quantity.

Results and discussion. The results of experiments to determine the width of the initial discharge window in the feed dispenser are presented in Figure 2. In this case, the amount of feed spilled per meter was measured when conducting experiments on the distribution of crushed corn by increasing the discharge window from 30 cm to 45 cm. Accordingly, when the width of the pouring window is 30 cm, the amount of corn on average is 3.18 kg/m, when it is 35 cm, the amount of feed is on average 3.64 kg/m, when it is 40 cm, the amount of feed is on average 4.71 kg/m, and when it is 45 cm, the amount of feed is it was found to increase to 6.26 kg/m on average (Fig. 2).

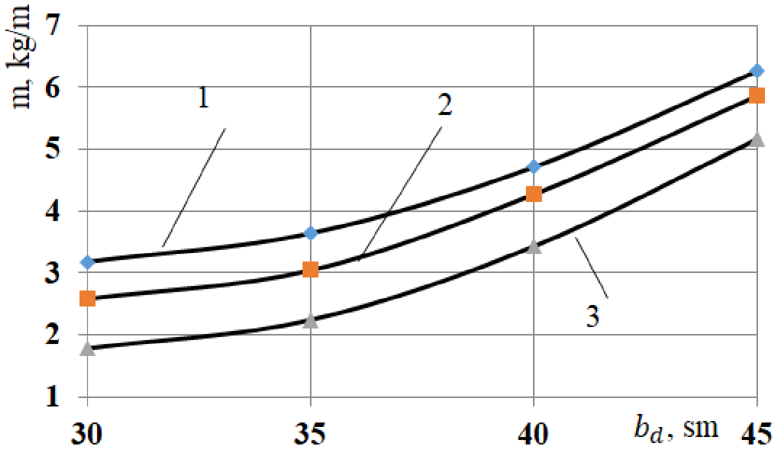

1) corn 2) alfalfa 3) straw

Figure 2. Coarse feeds depending on the width of the discharge window change in the amount of distribution

When the distribution of chopped alfalfa was studied in the same way, when the width of the pouring window was 30 cm, the amount of feed was on average 2.58 kg/m, when it was 35 cm, the amount of feed was on average 3.04 kg/m, when it was 40 cm, the amount of feed was on average 4.27 kg/m, 45 cm, it was found that the amount of feed increases to 5.86 kg/m on average (Fig. 2).

When studying the level of distribution of chopped straw as above, when the width of the pouring window is 30 cm, the amount of feed is on average 1.78 kg/m, when it is 35 cm, the amount of feed is on average 2.24 kg/m, when it is 40 cm, the amount of feed is on average 3.43 kg/m, 45 cm, it was found that the amount of feed increases to 5.16 kg/m on average (Fig. 2).

Based on the research, it was determined from the above experiment that the number of blades in the rotor is 2 pieces, the number of revolutions of the blade rotor is 50 r/min, and the height of the pouring window is changed from 20 cm to 35 cm when the width of the pouring window is 40 cm.

When the height of the discharge window is changed from 20 cm to 35 cm with 5 cm intervals, when the height of the discharge window is changed in the device, the average discharge mass of the ground corn when the height of the discharge window is 20 cm is 3.28 kg/m, and it is 3.39 kg on average when the height of the discharge window is 20 cm. /m was found to increase to an average of 4.35 kg/m at 30 cm and 5.49 kg/m at 35 cm (Fig. 3).

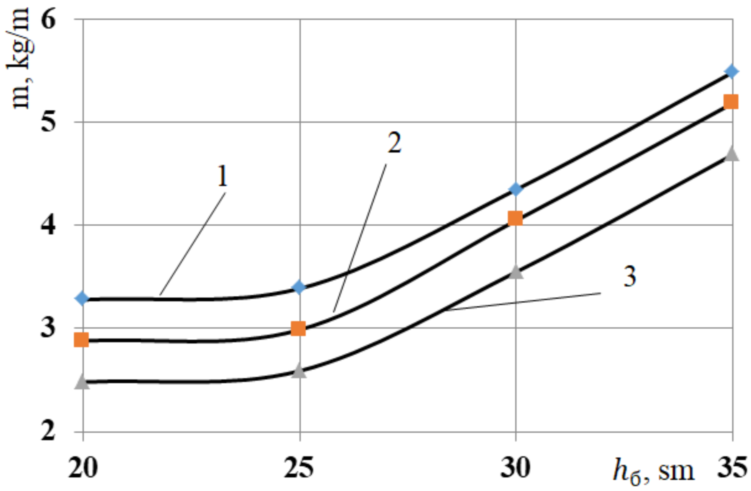

1) corn **2) alfalfa** **3) straw**

Figure 3. Coarse feeds depending on the height of the discharge window change in the amount of distribution

When analyzed in the same way, the mass of the crushed alfalfa was 2.88 kg/m on average, 25 cm on average 2.99 kg/m, 30 cm on average 4.05 kg/m, 35 cm on average 5.19 kg/m it was found to increase (Fig. 3).

Analyzes of chopped straw showed that the shed mass averaged 2.48 kg/m, 2.59 kg/m at 25 cm, 3.55 kg/m at 30 cm, and 4.69 kg/m at 35 cm. was determined (Fig. 3).

Conclusions. According to the results of the conducted experiments, in order to ensure the quality of distribution of coarse feed at the level of the specified requirements, the width of the discharge window of the distribution device should be 40 cm. In this case, the amount of feed spillage is 4.71 kg/m in corn, 4.27 kg/m in alfalfa and 3.43 kg/m in straw, which satisfies the initial requirements. The height of the pouring window should be 30 cm to ensure the required quality of pouring ground corn, alfalfa and straw. The amount of distributed mass is 3 kg to 5 kg per daily ration, 4.35 kg/m in corn, 4.05 kg/m in alfalfa, and 3.55 kg/m in straw, which is at the level of the specified requirements. According to the results of the experiment, the height of the discharge window of the developed distributor device was assumed to be 30 cm and the width was 40 cm.

References.

1. Karshiev F U, Mamatov F and G'apparov Sh 2022 *IOP Conference Series: Earth and Environmental Science* 1076 (1) 012024
2. F U Karshiev, Sh Ch Tursunov, A D Rasulov and D Kh Khudaynazarov IOP Conf. Series: Earth

and Environmental Science 1112 (2022) 012054
3. Borotov A 2021 *IOP Conference Series: Earth and Environmental Science* 868 012035
4. R K Choriev, D Khudaynazarov and D A Israilova IOP Conference Series: Earth and Environmental Science 213.230.109.7 on 23/08/2022
5. Alijanov D, Abdurokhmonov Sh, Jumatov Y and Bozorboev A 2020 *IOP Conference Series: Materials Science and Engineering* 883 012155
6. K D Astanakulov, G G Fozilov, N M Kurbanov, B Sh Adashev and S A Boyturayev 2020 *IOP Conf. Series: Earth and Environmental Science* 614 012129
7. Sattarov N E, Borotov A N, Yunusov R F and Yangiboev A E 2022 *IOP Conference Series: Earth and Environmental Science*, 1076 (1) 012081
8. Alijanov D and Jumatov Y 2022 *IOP Conference Series: Earth and Environmental Science* 1076 012063
9. Borotov A N 2022 IOP Conference Series: Earth and Environmental Science 1076 (1) 012027
10. F. M. Mamatov, E. Eshdavlatov, A. Suyunov, The Shape of the Mixing Chamber of the Continuous Mixer, *J Adv Research in Dynamical & Control Systems* 12, 2016-2023 (2020)
11. Mamato F. M., Eshdavlatov E., Suyuno A. Continuous Feed Mixer Performance, *Journal of Advanced Research in Dynamical and Control Systems* 12, 2195-2200 (2020)

AGRICULTURAL ENGINEERING SOLUTIONS
ISSN: 2181-399X Volume 3, Issue 3, 2023

RESEARCHING THE PARAMETERS OF THE WORKING BODY OF AN ENVIRONMENTALLY COMFORTABLE SPRAYING UNIT

Kh. Irisov[1] I. Bekmurodov[2]

[1] Tashkent State Agrarian University, University street 2, Qibray area, Tashkent reg, 100140, Uzbekistan
[2] University of Public Safety, Chorsu fortress, Zangiota district, Tashkent region, 100109, Uzbekistan

Abstract. In this scientific article, it is presented thet the general structure and operation process of the vibro-hydromachine, which is agrotechnically and ecologically convenient for the agro-industrial complex, does not cause chemical damage to other types of crops in the environment, and ensures that the spraying unit is energy-efficient. The theoretical aspects of determining the main parameters and operating modes of the vibrohydroelectric machine are given (velocity pressure of a hydraulic or pneumatic mixer and the potential energy of settling particles (or kinetic energy at the moment of settling), to ensure the circulation of mixing flows, the required flow rate of jets from the hydraulic mixer nozzles is, fluid pressure force at point A, pressure at point 2 at depth h, measured from the level of point 1, absolute pressure (P_a) at an arbitrary point in the liquid, excessive pressure P_i, flow of working fluid through the sawing device of the unit, insignificance h_e). Also, field experiments have shown the performance of the modernized proposed working bodies.

Key words: drops, working fluid, energy-saving, hydro-mixer, spraying, chemical damage

Introduction. The agricultural sector uses agrotechnical, mechanical, biological, chemical and physical methods of plant protection [1,2,3,4,5]. According to many scientists and specialists [6,7,8,9], the chemical method of plant protection in the near future still remains one of the main methods of protecting plants from various pests and diseases.

At the same time, the transition to a low-volume or ultra-low-volume spraying method is both economically and environmentally beneficial. Therefore, improving the design of modern spraying equipment is of great interest. Existing technical means have a high energy intensity of the spraying technological process and low technical efficiency of the working fluid used [10,11,12]. A large volume of supplied working fluid requires significant kinetic energy to crush it and transport the formed droplets to the surface of the object being processed.

Materials and methods. Hence the need arose to increase the technical efficiency of the formed droplets and reduce the energy intensity of the dispersion process by expanding the technological capabilities of the spraying unit.

To achieve this task, the authors have developed a new multifunctional spraying unit containing a vibro-hydro or pneumatic mixer 4, a rotary-roller dispenser 19, a reservoir 2, a control unit 16 with a distributor 14 and hydraulic communications 7 and 21 (Fig.1) [12].

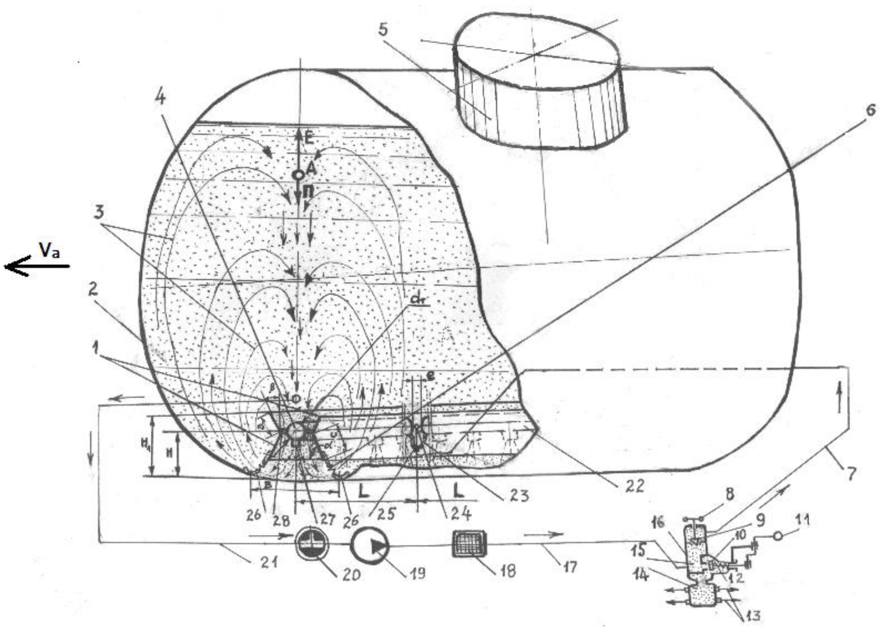

Fig.1. Scheme of the technological process of operation of the proposed vibrating hydraulic mixer: 1- fairings; 2-reservoir; 3 currents of working fluid; 4-vibrohydro-or pneumatic mixer; 5- neck; 6- spring-vibrator; 7,17,21,22,23,13- tubes; 8-valve; 9-bypass valve; 10-stop valve; 11-handle; 12-return spring; 14-distributor; 15-working cavity; 16- block regulator; 18-main filter; 19- rotary roller pump; 20-way valve; 24-hinge; 25-adapter; 26-foot; 27-spray; 28-perforated bracket; H, H_l, d, e, L, B, c, α, β - the main parameters of a vibrohydro or pneumatic mixer; V_a – unit speed.

The tank is equipped with a float dispenser. The dispenser is made in the form of two float elements 2, placed inside the tank with the possibility of free movement up or down along the rod 9 vertically lowered into the tank through its lid (Fig.2).

Unlike the well-known one, the proposed vibrohydro or pneumatic mixer consists of two folding parts. The hinged mount 24 greatly facilitates service work to eliminate sudden failures in a vibrohydro or pneumatic mixer. If necessary, the outlet pipe 21 can be directly connected to the aero-vortex caviator of the spraying unit. The hydraulic mixer can also operate in pneumatic mode.

Due to the constant circulation of the working fluid around the vibrating hydraulic mixer, conditions are created to ensure a constant concentration of the sprayed working fluid.

Results and Discussion. In the proposed vibro-hydro or pneumatic mixer, settling particles of the drug can be lifted upward under conditions if:

$$E \geq P, \tag{1}$$

where E, P – are the velocity pressure of the hydraulic or pneumatic mixer and the potential energy of the settling particles (or kinetic energy at the moment of settling), kgm^2/sec^2.

To ensure the circulation of mixing flows, the required flow rate of jets from the nozzles of the hydraulic mixer is equal to:

$$\upsilon_j = K_c \sqrt{\frac{M}{nd_{\text{n}}^2} C}, \tag{2}$$

where K_c – circulation coefficient, K_c=4.5; M – is the mass of the filling dose of the drug, kg; n – is the number of hydraulic mixer attachments; d_n – diameter of the nozzle hole, m; C – value is assumed to be constant for the operating conditions of the hydraulic mixer, m^6/kgsec^4 .

Springs - vibrator 6 imparting oscillatory movement on the body of the mixer 4 creates conditions for increasing the intensity of mixing the liquid in the tank.

The reservoir of the unit is equipped with a float dispenser 2 (Fig.2), which ensures the supply of a small portion of the working fluid by the air-vortex caviator.

So, for example, in a tank, on the surfaces of the float elements 2 there is a compression stress equal to:

$$P_{\underset{\lim \to \Delta S}{A}} = \frac{\Delta P}{\Delta S}, \tag{3}$$

where P_A – is the fluid pressure force at point A; ΔS – is the value of the elementary area containing point A; ΔP – compressive force acting on the area ΔS.

The pressure of the working fluid increases with depth h according to the law:

$$P_2 = P_1 + \gamma h, \tag{4}$$

where P_1 – is the pressure at an arbitrary point 1 of the liquid in the tank; P_2 – is the pressure at point 2 at depth h, measured from the level of point 1; γ – specific gravity of liquid (γ=1000 kg/m^3).

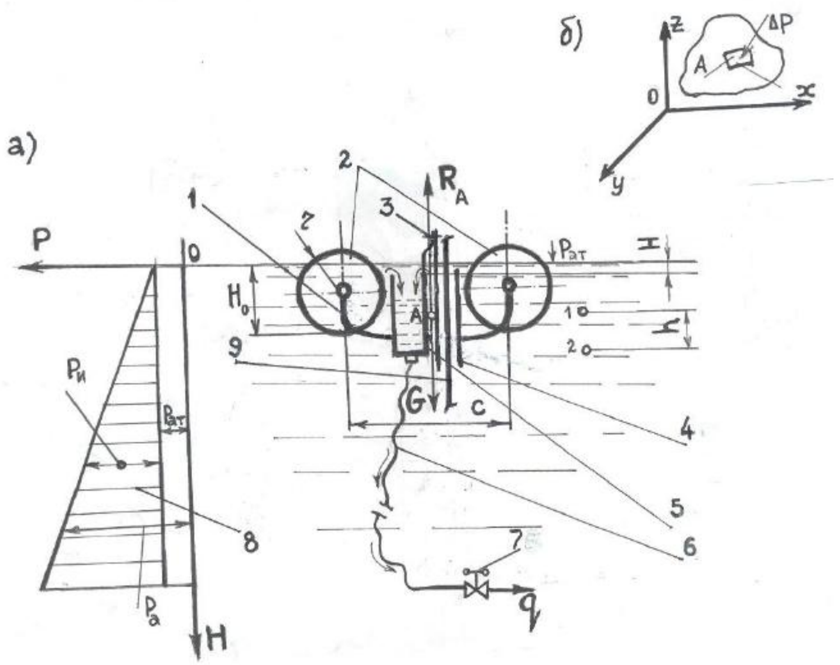

Fig.2. Scheme for calculating a float dispenser: 1- bracket; 2 - floats; 3-adjusting element; 4- bushing; 5- siphon; 6- tube; 7- valve; 8—fluid pressure diagram; 9- rod, b- coordinate axes of point A.

The absolute pressure (P_a) at an arbitrary point in the liquid is equal to:

$$P_a = R_{at} + \gamma H, \tag{5}$$

where H – is the depth of the point above the free surface; R_{at} – atmospheric pressure.

The excess pressure created in this case only by the volumetric weight of the liquid is equal to:

$$P_e = \gamma H\ . \tag{6}$$

As can be seen, by maintaining a constant depth h of sinking siphon 5 into the working fluid. Applying the theorem of momentum on the jet axis, we find the flow rate of the working fluid through the sawing device of the unit:

$$H\gamma F_c = q\rho\upsilon = f_j\upsilon^2\rho = \upsilon^2\frac{\gamma}{g}; \quad (7)$$

$$q = \mu_c f_c\sqrt{2gP_e}, \quad (8)$$

where f_j – jet cross section ($f_j = \frac{\pi d_c^2}{4}$); P_e – excessive pressure in the central tube at the level of the capillary channel of the caviator, ($H = \frac{P_e}{\gamma} = \frac{P_a - P_{at}}{\gamma}$); υ- the speed of the supplied jet, м/c; d_c^2 – diameter of the capillary channel; μ – capillary channel flow coefficient, (μ≈1,0); d_c – diameter of the capillary channel.

When using a pneumatic mixer, the tank of the apparatus transforms into a closed vessel with some excess pressure on the free surface ($P_o > P_{at}$) and the piezometric plane can be located above the free surface of the working fluid by the following amount:

$$h_e = \frac{P_o - P_{at}}{\gamma} = \frac{P_e}{\gamma}. \quad (9)$$

where P_e – excessive pressure on the free surface of the liquid.

However, due to the insignificance of h_{on} compared to h, it can be neglected in calculations.

The coaxially streamlined air flow created by the OVX-600M fan of the unit transports highly dispersed droplets formed by the sprayer to the object being processed.

Conducted field experiments showed the performance of the modernized proposed working bodies. The average median diameter of droplets formed is 99.79...104.05 microns at a working fluid flow rate of up to 75 l/ha (200 l/ha with the existing one), and the average level of leaf fall during cotton defoliation was 97.5% (80-90% with existing spraying method), which indicates the high efficiency of the modernized spraying unit.

Conclusion. Traditional spraying methods do not provide a low-volume supply of working fluid to the sawing tips.

The use of a vibrating hydraulic mixer ensures the stability of the concentration of the working fluid in the tank.

Equipping the unit with a vibrating hydraulic mixer and a float dispenser increases the technical efficiency of the sprayed liquid and makes the unit multifunctional.

The average median diameter of the formed drops was 99.79...104.05 microns at a working fluid flow rate of up to 75 l/ha (200 l/ha with the existing one), and the average level of leaf fall during the defoliation of cotton was 97.5% (80-90% with the known spraying method).

References.

1. Matchanov R, Rizayev A, Astanakulov K, Tolibaev A, Karimov N 2021 *IOP Conf. Series: Earth and Environmental Science* 677 1 – 6
2. F A Alimova et al 2022 *IOP Conf. Ser.: Earth Environ. Sci.* 1112 012021
3. Shaymardanov B, Borotov A and Jumatov Y *2020 IOP Conference Series: Materials Science and Engineering* 883 (1) 012111
4. Abdulkhaev Kh G and Barlibaev Sh N 2023 *IOP Conf. Ser.: Earth Environ. Sci.* 1154 012058
5. Kh D Irisov et al 2022 IOP Conf. Ser.: Earth Environ. Sci. 1076 012011
6. MireiaAltimira, Alejandro Rivas, Gorka S. Larraona, Raul Anton, Juan Carlos Ramos 2009

International Journal of Heat and Fluid Flow 30(2) 339–355
7. Gary J.Dorr, Andrew J.Hewitt, SteveW.Adkins, Jim Hanan, Huichun Zhang, Barry Noller 2013 CropProtection 53 109–117
8. Khmelev V N, Shalunov A V, Shalunova A V 2010 Alt. state tech. un-t, BTI Biysk 22 – 23
9. Borotov A, Choriev R, Boykulov U and Khatamov A 2023 E3S Web of Conferences 390 04038
10. Podgornyj Yu I *et al* 2021 *J. Phys.: Conf. Ser.* 2061 012039
11. Marko Petković *et al* 2021 E3S Web of Conferences 273 07028
12. Irisov Kh and Xamidov G 2023 *E3S Web of Conferences* 386, art. no. 03003.

AGRICULTURAL ENGINEERING SOLUTIONS
ISSN: 2181-399X Volume 3, Issue 3, 2023

RESERACHING THE CONTOUR AND DIMENSIONS OF THE GUIDING CHANNEL OF AN ELLIPTICAL DRUM ACCORDING TO THE OPERATION CONDITIONS AND KINEMATIC REGIMES

Sh. Ravutov[1*], G. Ibragimov[2], S. Shokirov[1], Sh. Komilov[1]

[1]Tashkent State Technical University, University Street-2, Tashkent, 700034, Uzbekistan.
[2]Department of Dynamical Systems and Their Applications V.I.Romanovskiy Institute of Mathematics Academy of Sciences of Uzbekistan 100174, Tashkent, Uzbekistan.

Abstract: In this article, it is described that the synthesis of the mechanism of an elliptical drum of a vertically spindle drum, which increases the completeness of the collection and the quality of the harvested raw cotton. In particular, it developed a methodology for substantiating the profile and dimensions of the guide track, which ensures the movement of the spindles along an elliptical trajectory. At the same time, the profile and dimensions of the guide track are considered as a function of the trajectory and kinematic modes of the spindle. It is shown that the trajectory of movement and kinematic modes of the center of the guide roller can be the basis for choosing the profile and basic geometric dimensions of the guide track. The trajectory of the center of the guide roller at its different positions relative to the center of the spindle, moving along an elliptical trajectory, is determined using the Geo Gebra program, which is popular in the mathematical modeling environment, and its kinematic parameters are determined by constructing hodographs of the speed of the center of the guide roller.

Key words: elliptical drum, vertical spindle, cotton harvester, kinematic regime, rotation

Introduction. One of the deficiencies of vertical spindle cotton harvesters (VS CH) used in Uzbekistan is low cotton harvesting completeness indicators at high yields (over 35-40 c/ha). According to many studies, the main reasons for this deficiency are the small number of spindles simultaneously participating in harvesting in the working zone and their low orientation to the cotton bolls [1, 2, 3].

Scientific research and experimental design work conducted since the creation of VS CH show that the complete elimination of this deficiency within the framework of a serial cotton harvesting apparatus is virtually impossible [4,5,6]. This is explained by the impossibility of directing the spindles along a given trajectory and controlling their kinematic regimes in a serial drum.

By structural design, a vertical-spindle drum is a planetary mechanism with reversible rotation of the satellites. And in terms of its construction, it consists of an upper and lower discs fixed to a shaft and equipped with vertical spindles mounted on the discs. During operation of the cotton harvesting apparatus, the shaft rotates along with the discs, and the spindles rotate around their own axes. The rotation of the spindles around their own axes in the harvesting zone is carried out by means of an immobilized friction belt installed externally, and in the cotton removal zone from the spindles by means of a reversing clutch immobilized internally inside the drum, which determines the reversible rotation of the latter. (Figure 1).

During machine operation, the spindles interact with the cotton bushes from the side and upon encountering cotton bolls, capture cotton locks, wind them around themselves and by rotating together with the drum and around their own axes, transfer the cotton windings to the cotton removal zone, where as a result of reversing the rotation direction, the main part of cotton self-falls off and is partially removed with the help of a brush picking head.

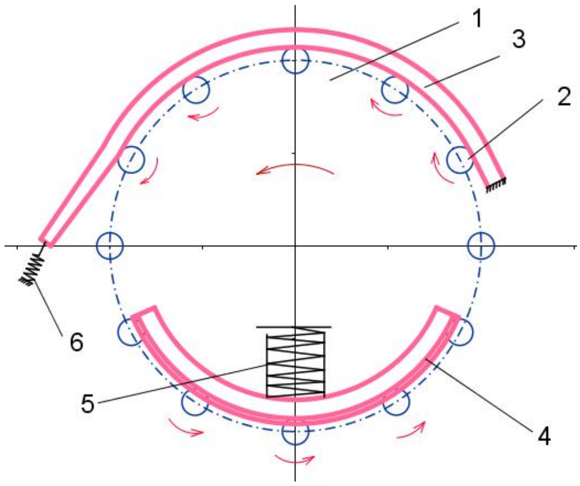

Figure 1. Scheme of a serial vertical-spindle drum: 1-drum; 2-spindle; 3,4-friction drives of the spindles; 5,6-springs

The effectiveness of spindle contact with bolls, encountering cotton, its capture and winding depends on the number of simultaneously operating spindles, their trajectory and kinematic regimes. At the same time, the process of interaction between spindles and cotton bushes has a probabilistic character: increasing the contact zone with cotton bushes and the number of simultaneously operating spindles, achieving optimal kinematic regimes of spindles should increase the efficiency of vertical-spindle drums [3].

Taking into account the impossibility of controlling the trajectory and kinematic regimes of spindles in a serial drum, the idea was put forward to control the trajectory and kinematic regimes of spindles through the structural development of the vertical-spindle drum mechanism [3]. According to this idea, each spindle on the drum must be installed on a separate cassette and must move in relative motion, forming a larger arc. Thereby, the contact zone of spindles with bushes increases and the number of simultaneously operating spindles in the working zone, and the kinematic regimes of the latter provide reliable wrapping and winding of cotton locks on the spindles. Drums created on this principle can be called non-circular, and the trajectories of relative spindle motion can be an ellipse or elongated oval, with the major axes coinciding with the direction of machine movement [3]. Issues of structural analysis of the mechanism of a non-circular drum, selection of basic kinematic regimes of mechanism links applicable to a cotton harvesting apparatus drum are considered in work [8]. The geometric and speed parameters of a non-circular (elliptical) drum, based on the working conditions of the cotton harvesting apparatus, are substantiated in work [3].

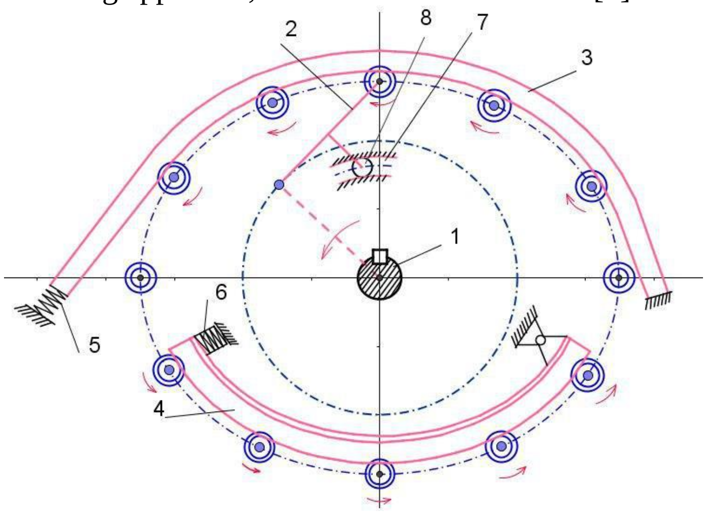

Figure 2. Diagram of the structurally developed (elliptical) drum: 1-shaft; 2-spindle cassette; 3;4-friction drives of the spindles; 5;6- springs; 7-guiding channel; 8-guiding roller.

Materials and methods

The theoretically substantiated geometric dimensions of the elliptical drum [3]: the major semi-axis b = 175 mm; the minor semi-axis a = 146 mm (equal to the radius of the serial drum); the length of the crank and the connecting rod are respectively equal to r = 105 mm and l = 100 mm; overall dimensions of the guiding channel are chosen constructively to provide easy installation of the reversing clutch on the drum. The determining factor in selecting the dimensions and shape of the guiding channel is the distance from the central line of the connecting rod to the center of the guiding roller. In work, [3,5,6] this distance is selected based on design considerations, determined as a perpendicular drawn from the center of the connecting rod and is m = 35 mm.

This work examines the change in shape and dimensions of the guiding channel depending on the change in the distance between the center of the connecting rod and the center of the guiding channel and studies their influence on the kinematic motion modes of the guiding roller. Recommendations are given for selecting the dimensions and shape of the guiding channel for designing an experimental elliptical drum.

To study the dimensions and shape of the guiding channel, we will use the “GeoGebra” program, which has now gained wide distribution in the field of mathematical modeling and is successfully applied to study technical systems and mechanisms [8]. The program allows accelerating the modeling of technical systems, visually observing the final result by varying the geometric dimensions of the system elements. For this, it is enough to enter two or several important points of the main link of the mechanism into the program editor. In our case, the important link of the mechanism is the connecting rod (section AC), one point of which (point A) is hinged to the crank (section AO) and describes a circle, and the other point (point C) a freely rotating spindle is installed, the center of which describes an ellipse. By connecting any point of the link to these points, it is possible to obtain the virtual trajectory of this point, while the motion of the important points can be animated (Figure 3).

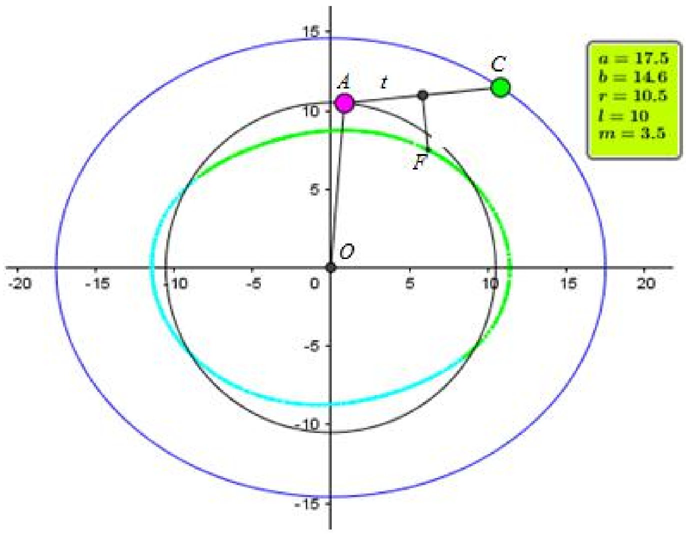

Figure 3. Formation of trajectories of main points of the mechanism of an elliptical drum using the “GeoGebra” program: the blue line is the trajectory of the spindle center; the green (light blue) line is the trajectory of the guiding roller.

Results and discussion. Fig.3 shows that during the elliptical movement of spindle center C, the movement of guiding roller center F occurs along a line different from an ellipse (quasi-ellipse). The shape of this line depends on the location of point F relative to points A and C. Point F can be located on line AC or outside it (Fig. 4). In the first case, as point F approaches point A, the trajectory shape also approaches a circle, and when approaching point C, naturally, an ellipse. In the case when point F is outside the line AC at a distance m, the trajectory of point F acquires the shape of a distorted circle (Fig. 4, t = 0) when approaching point A, and a distorted ellipse (quasi-ellipse) (Fig. 4, t = 50) when approaching point C. The second case for the mechanism of an elliptical drum is accepted for constructive reasons to provide sufficient space for installing and servicing the reversing clutch in the cotton removal zone from the spindles. In the adopted design of the cotton harvesting apparatus with elliptical drums, the reversing clutch of the spindles, as in the serial drum, is installed in the internal contour of the drum. Therefore, point F is located in the inner part of the drum contour, forming an arm of length m. From constructive considerations, the maximum offset of the arm m from point A is accepted as the middle of line AC (t = 50 mm), since further approximation of the arm to point C leads to a reduction in space for installing the reversing clutch.

Obtaining the trajectory of motion for point F by animating the mechanism in GeoGebra program allowed visually observing the change in shape of the guiding roller center trajectory depending on the location of arm m relative to points A and C. The observation was carried out by varying the distance t in 10 mm intervals with a constant arm length of m = 35 mm. Fig. 4 shows some contour views of point F's trajectory. Thus, at t = 0 the contour of point F's trajectory is close to a circle, with small changes in curvature radius in some areas. But with increasing t, the intensity of changes in curvature radius increases (t = 20 mm), at t = 30 mm, areas close to a straight line appear, and further increasing the distance t is accompanied by the formation of a trajectory close in shape of an ellipse.

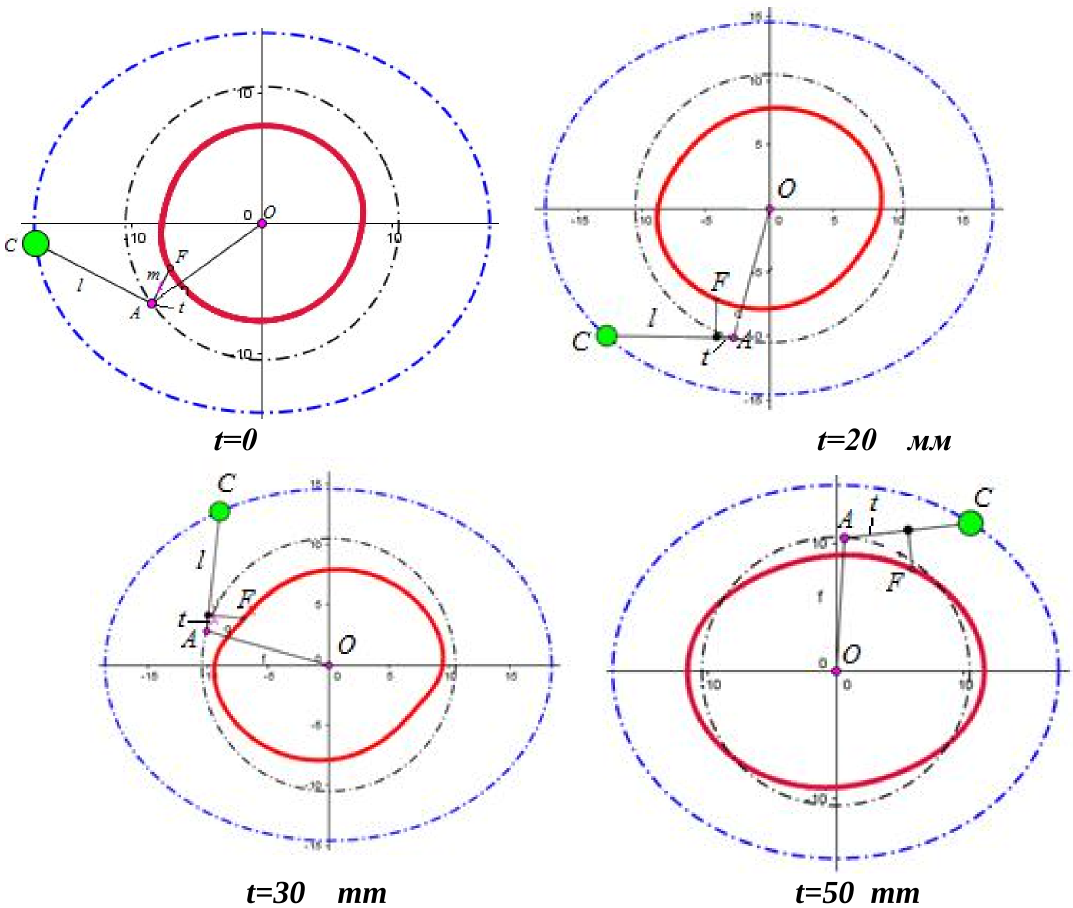

Figure 4. Change in the trajectory of the guiding roller center F depending on its location relative to link AC.

The influence of changing the length of the arm m on the dimensions and shape of the guiding channel was also studied. The results show that increasing the length of the arm m leads to a decrease in the dimensions of the guiding channel, but at the same time there is an increase in the difference of curvature radius in its individual sections.

For an objective assessment of the influence of the shape and dimensions of the guiding channel on the operation of the guiding roller in an elliptical drum, it is necessary to study the kinematics of the important points of this mechanism, including the guiding roller (point F).

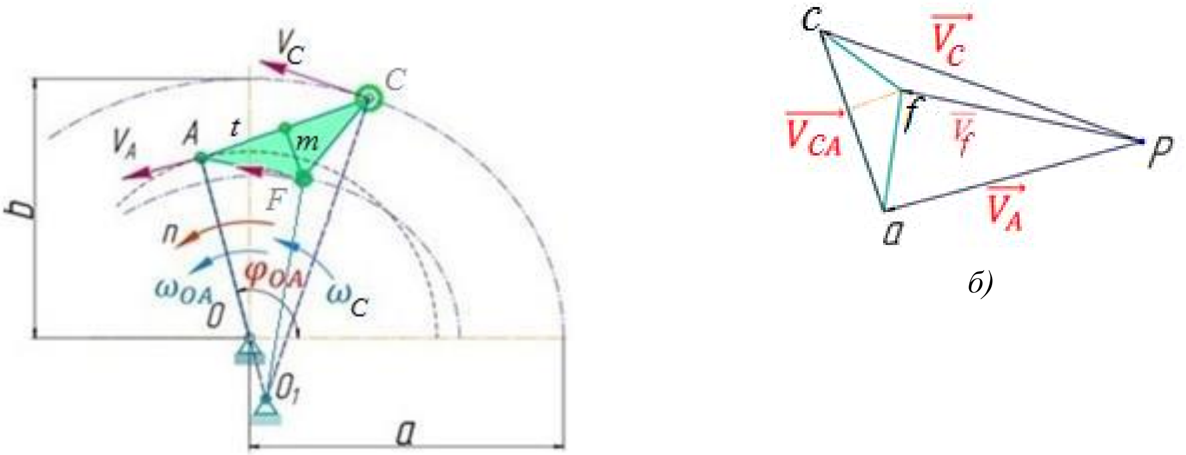

a)

б)

Figure 5. a - the mechanism of the elliptical drum; b - the speed plan of the mechanism.

For studying the kinematics of point F, it is convenient to apply the method of constructing speed plans of the mechanism [6] (Figure 5). The convenience of this method is due to the speed and visibility of solving applied design problems. In addition, graphical methods are distinguished by the convenience of controlling the obtained results.

To assess the laws of variation in magnitude and direction of velocities of mechanism links' points, vector hodographs of their velocities are often used. They stand out for their high visual clarity of results and are usually more convenient than plotting graphs [6]. This approach, besides its visual appeal, allows for easy determination of the direction of the acceleration vector of a point in a given position. Considering these advantages of the method for assessing the intensity of velocity variations in the center of the guide roller, we will make use of the hodograph of velocities.

The calculations were performed at different values of m and t. Table-1 presents the results of calculation-graphical work for constructing hodographs of the velocity of point F at m values of 30, 40, and 50 mm, as well as at t values of 0 and 50 mm. The first row of the table illustrates the fixation of the arm m at point A. As can be seen from the diagrams, as the length of the arm changes from 0 to 50 mm, the intensity of the velocity variation of point F increases. For example, at t = 0 and m = 40-50 mm, a loop is formed on the hodograph of velocities, which is undesirable from the standpoint of the dynamics of the mechanism's operation. Moving the arm away from point A towards point C leads to a decrease in the intensity of the velocity variation. Particularly, at m = 30 and t = 50 mm, a smoother change in the velocity of point F is observed (Table 2).

Table 2. Hodographs of the velocity vectors of point F.

	m=30	*m=40*	*m=50*
t=0	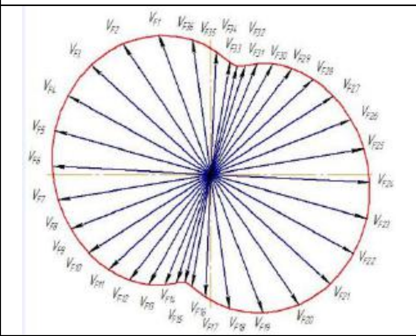	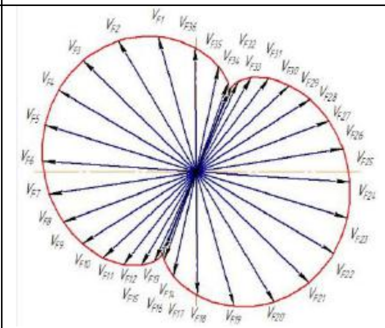	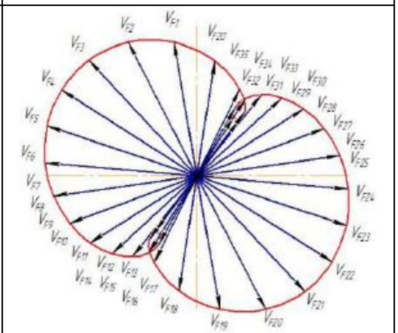

t=50

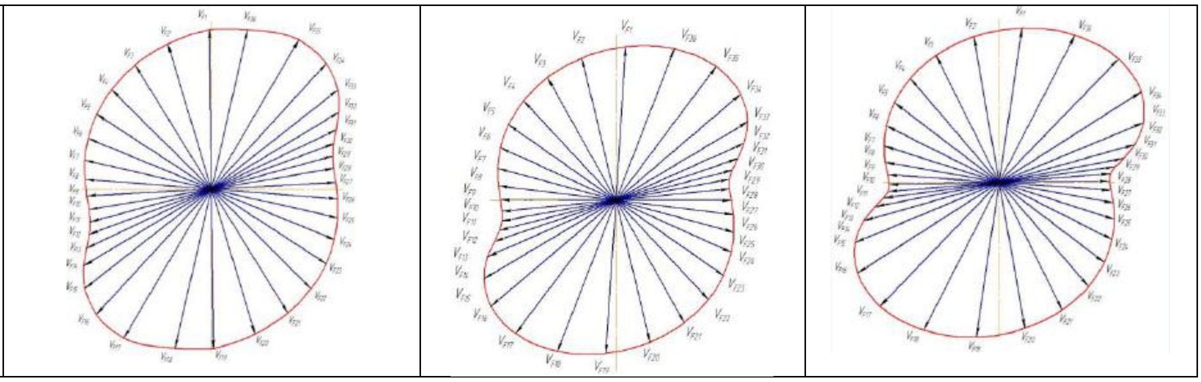

Conclusions. An effective methodology for studying the changes in shape and size of the guide track of an elliptical drum mechanism, depending on the position of the center of the guide roller, has been developed using the "GeoGebra" software. Additionally, a methodology for studying the kinematics of the guide roller of the elliptical drum has been developed. The obtained results allow for the selection of rational dimensions for the guide track of the elliptical drum in the initial stage of its design. These results also indicate the need for further research in studying the dynamics of the elliptical drum mechanism.

References.

1. Sablikov V M Cotton harvesting machines.–M.: Agropromizdat, 1985.–152 c.
2. Glushchenko A.D., Rizaev A.A. Modeling of dynamic interactions of cotton lobes and spindles in cotton harvesters. *Fan*, 1995, 131 h.
3. Rizaev A A et al Cotton harvesters for one-time cotton-picking. *Mater. Sci. Eng.* 2021,1030,012173. [CrossRef]
4. Turanov Kh, Abdazimov A, Shaumarova M., Siddikov S Incorrect application of the epicycloid equation to the planetary mechanism of a vertical spindle of the cotton harvester. *E3S Web of Conferences* 164, 01008 (2020). doi: 10.1051/e3sconf/202015701008
5. Ravutov Sh T, Rizayev A A, Rajapbaev U A On the issue of incrasing the efficiency of the spindles of a vertical-spindle cotton picker. *IOP Conf. Series: Earth and Environmental Science* 1112 (2022) 012043.
6. Bahodirov G, Ravutov Sh, Abdukarimov A, Toshmatov E Development of the metods of kinematic analysis of elliptic dram of vertical-spindle cotton harvester. *IOP Conf. Series: Materials Science and Enjineering* 1030 (1), 012160.
7. Ermakov B.E., Asriants A.A. and others. Theoretical mechanics: theory, tasks and examples of problem solving. *Textbook for technicians. Universities, Mashinostroyeniye*.: 2007. – 344 c
8. http://creativecommons.org/licenses/bv-nc-sa/3.0/

AGRICULTURAL ENGINEERING SOLUTIONS

ISSN: 2181-399X Volume 3, Issue 3, 2023

RESEARCHING THE PARAMETERS OF THE COMB FOR LAYING THE DRIP IRRIGATION HOSE AND SOWING SEEDS

B. Shaymardanov[1*], P. Berdimuratov[2], D. Ruziev[3] and A. Rakhimov[3]

[1,2,3] "Tashkent Institute of irrigation and agricultural mexanization engineers" National Research University " National Research University, 39, Kari-Niyaziy, Tashkent 100000, Respublika Uzbekistan

[3] PC “GSKB-Agromash” chief designer, 210, Mashxadiy, Tashkent 100000, Respublika Uzbekistan

Abstract. In this article it is presented that the results of the reserach on the formation and justification of the parameters of a comb for laying a drip irrigation hose and sowing seeds. The features of the agrometeorological conditions of Uzbekistan during spring sowing are studied. Based on the variability of weather - precipitation, atmospheric air temperature and soil, the parameters of the ridge size are justified. The design of the machine for pre-sowing strip milling of the soil, the formation of the ridge, the laying of the drip irrigation hose, soil compaction, providing physical and mechanical soil of the ridge and the possibility of sowing seeds, is proposed. The design of a milling machine for strip processing with the formation of a ridge of a given shape, composition and parameters, a ridge sealer according to the required soil density has been developed. The main parameters of the comb shaper are substantiated.

Key words: drip irrigation hose, comb, pre-sowing, rain stream, deterioration, soil crust

Introduction. Features of agrometeorological conditions of Uzbekistan during spring sowing. For this purpose, materials of the Uzhydrometeorological Center were collected from March 25 to April 25 in recent years on air temperature, soil and precipitation in the Tashkent and Andijan regions.

A very important factor here is the amount of precipitation and their intensity during the sowing period, since the appearance of a soil crust over the seedbed, the source of re-sowing, depends on it.

1), the greatest amount of precipitation from 91.1 to 153.7 mm and its intensity from 13 to 21 days occurred in the period 2010-2012. It is known that as a result of high intensity and a large amount of precipitation, the seedbed is flooded by rain streams, which contributes to the formation of a soil crust and, accordingly, the deterioration of the development of seedlings. The results of this analysis are shown in Fig.1.

From Fig. 2 it can be seen that due to the formation of a soil crust 4 on the field 2 above the seedbed 3, after precipitation, the seeds die.

In recent years, the Republic has started using crops on ridges cut in autumn to protect crops from rain flows, exclude replanting, and, accordingly, increase crop yields. However, in order to carry out sowing using this technology, it is necessary to cut the ridges in the fall on the field, and before sowing, prepare the top of the ridge for this operation, which requires at least two separate units, which increases operational and labor costs by 3-3.5 times. In addition, during this period of time there were years with a small amount of precipitation (2000, 2001, 2004, 2008) (from 17.2 to 37.4

mm) and their intensity (from 4 to 8 days). This amount of precipitation is insufficient for the normal development of seedlings. To eliminate this phenomenon, it is necessary to carry out feeding irrigation with a small amount using drip irrigation [1-7].

It follows from this that in order to eliminate excess moisture or its insufficiency, it is best to sow cotton on ridges formed simultaneously by laying a drip irrigation hose, which will allow for less cost and in a short time to eliminate the effects of precipitation on seedlings and protect them from rain flows and, if necessary, carry out feeding irrigation.

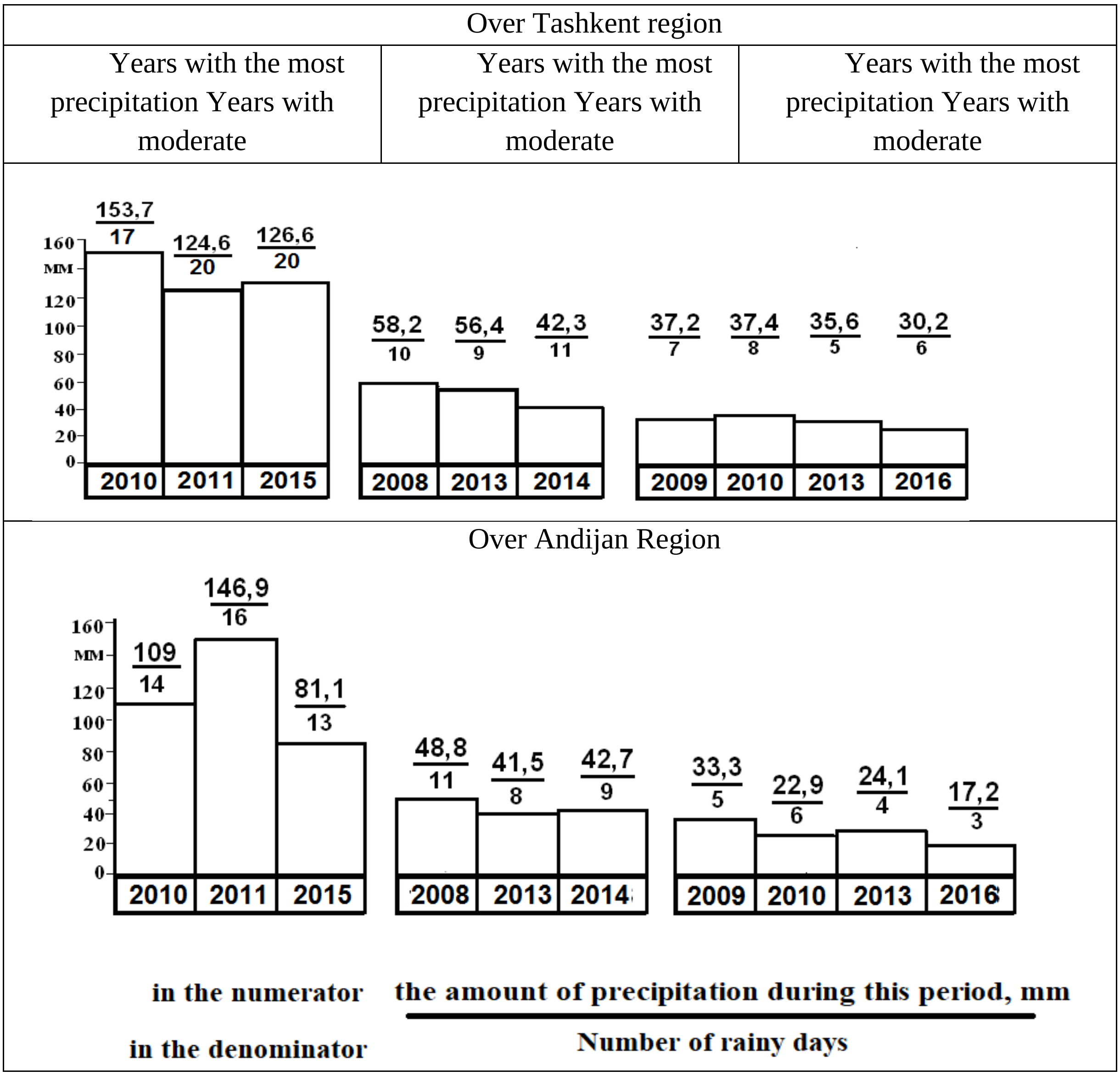

Fig.1. Precipitation and its intensity during the cotton sowing period for 10 years (from March 25 to April 25) according to the data of Uzhydromet

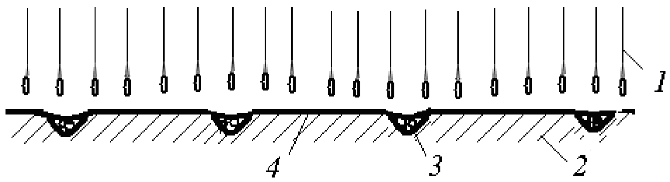

Fig.2. Sowing on a smooth floor (traditional method of sowing)

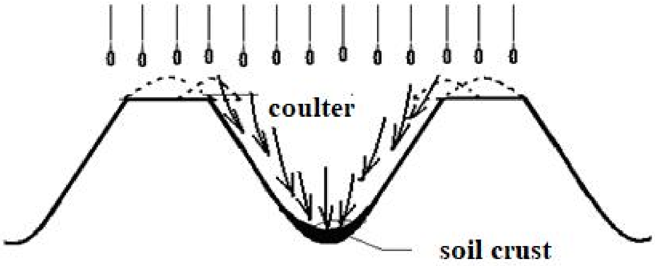

Fig.3. Scheme of formation of soil crust on the sides of the ridges when sowing cotton on the removed ridges

The second important factor for the emergence of seedlings is the temperature of the soil and air. So at a soil temperature of 10-120C, the awakening of the vital activity of cotton seeds begins, at 13-140C the embryo begins to grow, at 14-160C seed germination begins, and at 17-180C the emergence of seedlings on the soil surface is ensured. At the same time, the difference between daytime and nighttime temperatures ranges from 9 to 160C, at night the temperature difference between adjacent calendar days is only 2-40C. While in the daytime it ranges from 3 to 60C.

According to the data, it can be seen that at night in a favorable for cotton growing in 2005, the minimum air temperature at night was from 7 to 140C, and in the same period in an unfavorable 2003 it ranged from 1 to 90C, that is, below 2005 by 5-60C, and during daytime in 2005 it fluctuated from 15 to 190C, that is, above the temperature of 2003 by 3-60C, (Fig.4).

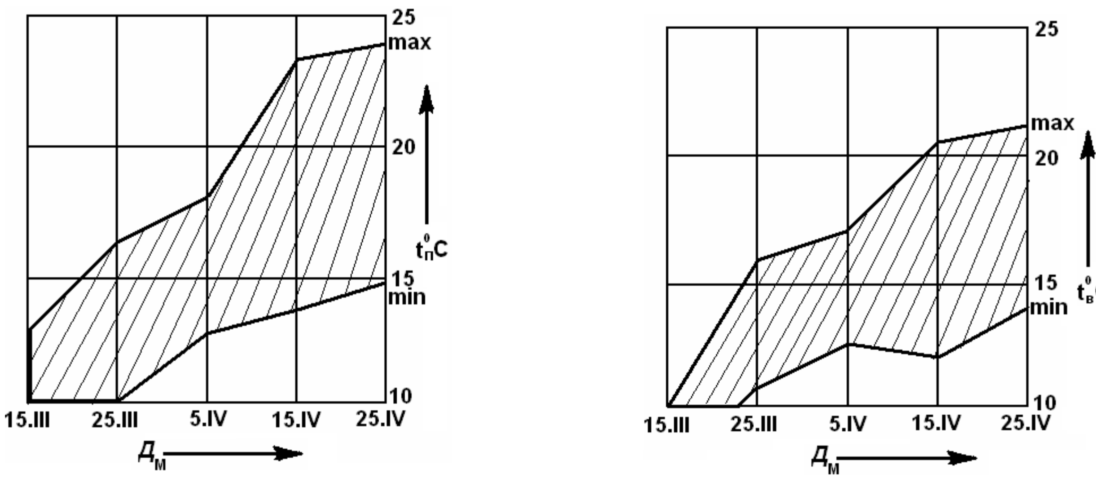

Fig.4. Average daily air temperature ($t_в$) and soil surface ($t_п$) from March 15 to April 25 (DM) for the last 10 years

It follows from this that an increase in air temperature and, accordingly, soil temperature allows sowing at an early date, which contributes to the production of healthy plant seedlings. The results of experimental studies show that with comb sowing on the soil layers of the root system of plants, the temperature increases. This is explained by the difference in the heat capacity of different bodies, for example, the heat capacity of air is 1.0, and for water it is 4.19. Hence, if we take into account that the driving force is considered to be the heat of the body, determined by the formula

$$Q = Mct, \ \ kJ \ ,$$

where Q– the amount of heat to the root system, KJ ; c – body heat capacity, kJ/kg gr; for air c_v =1 kJ/kg *gr; for water c_v = 4,19 kJ/kg gr; t – soil temperature, ^{0}C.

To eliminate the harmful effects of risky weather conditions on cotton crops, first of all, it is necessary to eliminate the ingress of rain flow into the seedbed. With this technology, cotton seeds will be embedded in a wetter and warmed soil than when sown on a leveled surface. This makes it possible to improve the quality of seedlings and plant development and thereby increase the total crop yield and shift the sowing time by 3-4 days.

Materials and methods. Problem statement - development of a milling machine for strip processing with the formation of a ridge of a given shape, soil composition and parameters, a ridge sealer for a given soil density.

A combined machine has been developed for pre-sowing strip milling of the soil with simultaneous laying of drip irrigation hoses and the possibility of sowing seeds (Fig.5). The machine consists of two parts: a comb cutter and a seeder.

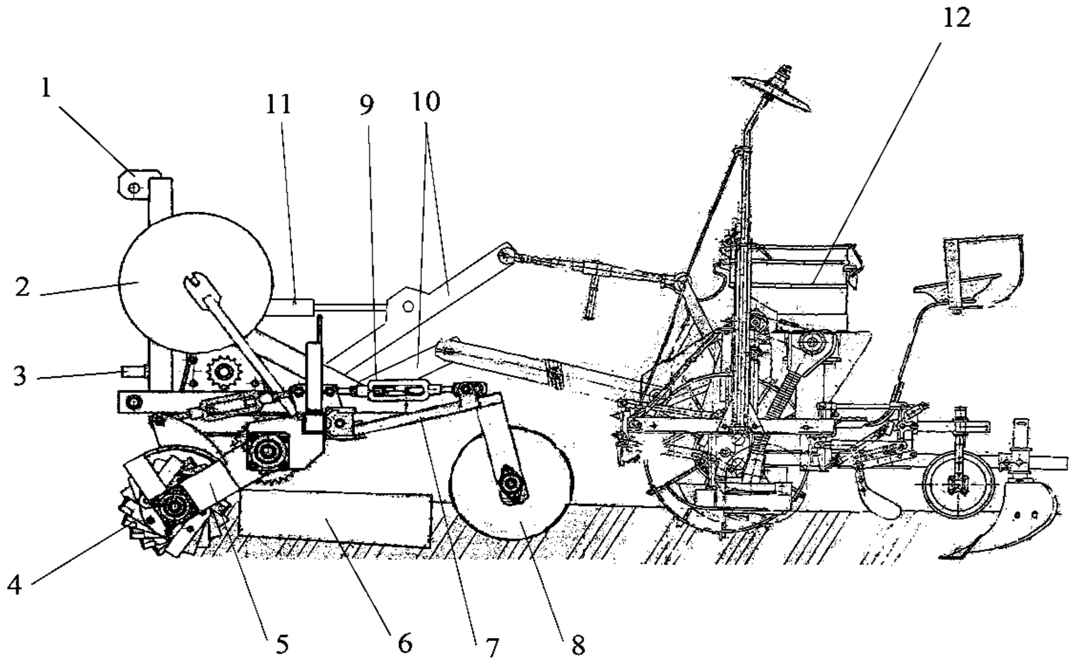

Figure 5. Combined machine for pre-sowing strip milling with simultaneous laying of drip irrigation hoses and the possibility of sowing: 1- milling cutter frame; 2-babina for drip irrigation hoses; 3-milling cutter drive gear shaft; 4-cutter knife drum; 5-knife drum bracket; 6-comb-forming apron; 7-comb bracket-a sealing roller; 8-a comb-sealing roller; 9-a turnbuckle for adjusting the sealing roller; 10-a mounted device for a seeder; 11-a hydraulic cylinder of a mounted device for a seeder; 12-a seeder.

The machine works as follows. In the period of preparation for sowing seeds, instead of harrowing and milling, the soil is milled with the simultaneous formation of a ridge of a given shape and the laying of drip irrigation hoses. Then the soil is compacted to the required density.

When milling, the crusts of the soil are deformed and its wet and dry components are mixed, thereby ensuring the uniformity of the mechanical composition and humidity. In years of insufficient moisture in the soil, immediately after sowing, absorbent irrigation is carried out using drip irrigation.

Results and discussion. Justification of the shape of the profile and the parameters of the ridge. In many regions of the Republic, one of the main requirements for the parameters of the ridge is the ability to protect the seedbed from flooding by rain flows and, consequently, to protect it from crust formation. During the operation of the cutter, ridges are formed, the walls of which crumble at an angle of natural slope. At the same time, the angle of natural slope of gray-earth soils prepared for sowing when it is filled with an increase in soil moisture from 7 to 18% increases from 32 to 410. Consequently, when the soil is poured into the field, ridges are formed in the form of an isosceles triangle. However, for the working bodies of seeders to work on top of such a ridge, it is necessary to have a platform with a width of 160-170 mm. To do this, the top of the ridge is sealed with a trapezoid shape seal along the longitudinal section, therefore, after that, such a ridge turns into an isosceles trapezoid before sowing (Fig.6). This form, which we take as the basis for subsequent calculations.

To determine the minimum permissible parameters of the ridge formed during sowing, we proceed from the fact that they are not flooded by rain streams. Such ridge parameters will be acceptable for gray-earth soils in the old irrigation zone of our republic, where the fields have a sufficient slope and a fertile soil layer.

The main parameters of the ridge include the width of the lower base bg, the width of the vertex bg, the angle of inclination of its wall to the horizon and the height of the ridge H. From Fig.2.3 it can be seen that to ensure the protection of the seedbed, the cross-sectional area of the row spacing groove SSDKM should be greater than the cross-sectional area of precipitation in the row spacing per day (QsVm). According to the data of the Uzbek Hydrometeorological Center for the last ten years in April, up to 34 mm of precipitation fell in the Tashkent region as much as possible per day.

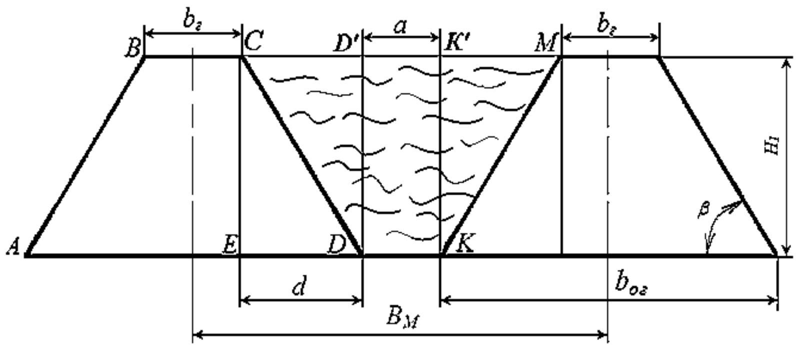

Fig.6. Scheme for determining the parameters of the ridge

To determine the parameters of the ridge, we assume that the precipitation should be placed in the groove of the row spacing, i.e. in the space between adjacent ridges. From here

$$B_м Q_c = S_{СДКМ}. \tag{1}$$

From Fig.6 we have

$$S_{CDKM} = S_{CDD'} + S_{D'K'KD} + S_{K'MK}, \tag{2}$$

где $S_{CDD'}$,$S_{D'K'KD}$ и $S_{K'MK}$– accordingly , the area of the triangles *CDD'*, *K'MK* and a rectangle *D'K'KD.*

From Fig.2.3 we have

$$S_{CDD'} = S_{K'MK} = \frac{1}{2} dH_1 = \frac{H_1^{\ 2}}{2} ctg\beta, \tag{3}$$

$$S_{D'K'KD} = aH_1, \tag{4}$$

where H_1 is the minimum allowable height of the ridge; β is the angle of the natural slope of the soil;

a is the width of the bottom of the groove.

The width of the bottom of the groove a is equal to

$$a = B_M - b_г - 2H_1 ctg\beta, \tag{5}$$

where bg is the width of the crest vertex.

Substituting the value of a in (4) we have

$$S_{D'K'KD} = (B_M - b_г - 2H_1 ctg\beta)H_1 \tag{6}$$

Substituting the values (3) and (6) first into (2), and then the resulting result into formula (1) we will have $B_M Q_c = H_1(B_M - b_г) - H_1^{\,2} ctg\beta.$ (7)

Having made the transformation of this formula, we obtain the following equation

$$H^2 - (B_M - b_г)H_1 tg\beta + B_M Q_c tg\beta = 0. \tag{8}$$

Having solved equation (8), we obtain the following dependence for determining the minimum allowable height of the ridge

$$H_1 = 0{,}5\left[(B_M - b_г)tg\beta - \sqrt{[(B_M - b_г)tg\beta]^2 - 4Q_O B_M tg\beta}\right] \tag{9}$$

When cutting the ridge, its side walls crumble at the angle of the natural slope β. At the same time, the soil moisture prepared for cutting the ridge usually ranges from 12 to 14%, and depending on this, the angle of the natural slope β varies from 32 to 41 °. Based on this, the minimum calculated height of the ridge H, as can be seen from the formula (9), practically very little depends on the magnitude of the angle of the natural slope β, as well as on the size of the top of the ridge bg and is mainly determined by the amount of precipitation that fell during the day Qc.

Taking Qc = 34 mm, bg = 160 mm, h = 36 mm and β = 36 ° and using formulas (9) we get that at Vm = 900 mm the height of the ridge H1 = 45.1 mm, and at Vm = 600 mm the height of the ridge H1 = 56.2 mm.

As is known, under the influence of precipitation, the ridge settles. At the same time, as studies have shown, the coefficient that takes into account the shrinkage of the soil, depending on the height of the ridge, is Cu = 0.85-0.90. The actual minimum allowable height of the ridge also depends on the height of the irregularities of the surface of the field h, which is on average 30-40 mm. With this in mind, the actual minimum height of the ridge H1 in order to protect its top from the rain flow should be equal to:

$$H_1 = \frac{1}{2K_y}[(B_M - b_г)tg\beta - \sqrt{[(B_M - b_г)tg\beta]^2 - 4Q_c B_M tg\beta}] + h, \tag{10}$$

Taking into account this formula and the above data,

by $B_м$=900 mm $H_1 = \frac{45{,}1}{0{,}9} + 36 = 86{,}1$mm; при $B_м$=600 mm $H_1 = \frac{56{,}3}{0{,}9} + 36 = 98{,}6$mm.

From these data it follows that rainwater does not flood the top of the ridge, its height should be practically at least 100 mm. In this case , the width of the lower base of the ridge will be

$$b_{ог} = 2H_1 ctg\beta + b_г. \tag{11}$$

The cross-sectional area of such a groove

$$S_г = (B_м - b_{ог})H_1 + H_1^{\,2} ctg\beta. \tag{12}$$

Substitute the above values into these expressions and the values H1, β, bg, Vm are obtained, we get $b_{ог}$= 435,28 mm и $S_г$=306 sm^2 при $B_м$=900 mm и 204 sm^2 при $B_м$=600 mm.

Thus, the calculations show that in order to eliminate the ingress of rain flow into the seedbed, it is necessary: the minimum allowable height of the ridge H1 should be at least 100 mm; minimum allowable width of the crest vertex $b_г$ from the point of view of stable operation of seeding devices should be at least 160 mm; permissible width of the lower base of the ridge $b_{ог}$ must be at least 435 mm; дpermissible cross-sectional area of the groove $S_г$ must be at least 306 sm^2 by B_m=900 mm and 204 sm^2 by B_m=600 mm.

Justification of the main parameters of the comb shaper. The main parameters of the shaper are the width of the input and output edges of the shaper's slide, the angle of installation of the side dumps to the direction of movement α and to the horizontal plane β_y, length of the slide L, side blade length $L_{бо}$.

During operation, the side dumps of the mold impact on the soil produce soil deformation (Fig. 6). At the same time, soil particles move laterally upwards.

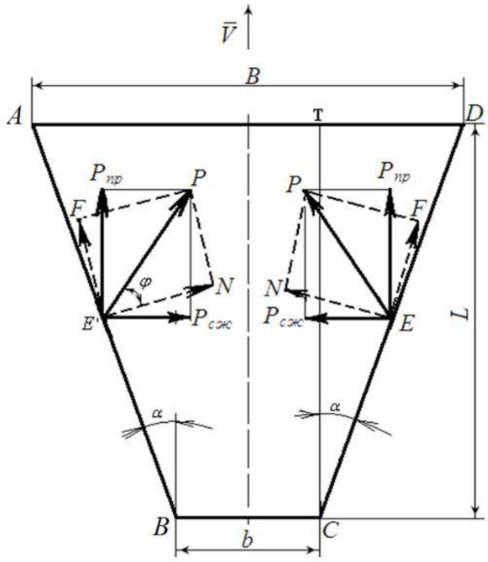

Fig.6. Scheme for determining the angle of installation of side dumps to the direction of movement

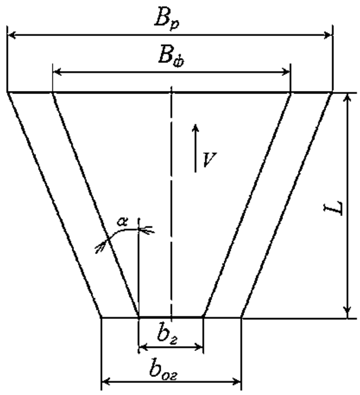

Fig.7. Scheme for determining the length of the shaper (L)

Angle of inclination of the side face of the ridge (β_y) (fig.8) depends on its compaction. If the angle of the natural slope of the soil on the side face , depending on humidity , varies from 32^0 to 41^0, and with its sealing , the angle β_y can be increased to 42^0-45^0 .

Substituting in (13) a known value φ=30^0, we get $\alpha \le 30^0$. Based on research on the choice of seal parameters, we accept α=14-16^0. By α=14-16^0 the soil slides along the side blade of the shaper and compacts the soil sufficiently to form a stable ridge.

From Fig. 7 we have

$$L = \frac{1}{2}(B_p - b_{oz})ctg\alpha \tag{14}$$

and

$$B = 2Ltg\alpha + b_z. \tag{15}$$

Substituting in (14) and (15) the values B_p, b_{oz} and α we get, that the length of the shaper should be within L = 183–238,9 mm, and the width of the shaper's entrance apron B=292-334 mm.

As a result of studying the method of forming a platform for the work of the working bodies of sowing machines, it was revealed that it was necessary to seal the side face of the ridge in order to eliminate its shedding. To do this, it was necessary to fulfill the following condition, so that the angle of the slope β_y to the plane of the field was no more than

$$\beta_y \leq \beta + \varphi \ , \tag{16}$$

where φ– the angle of internal friction of the soil; β – angle of natural slope of the soil.

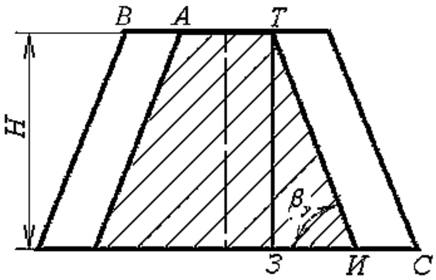

Fig.8. Scheme to substantiate the angle of installation of side dumps to the horizon

Based on this, in order to eliminate the shedding of the side faces of the ridge, it is necessary to place the side dumps of the shaper at an angle $\beta_y = 42 - 45^0$ to the horizontal plane of the field.

When working, the visor of the shaper's apron affects the soil and causes soil deformation. Installation angle α_1 the apron visor will be determined from the condition of ensuring the sliding of the soil on it, i.e..

$$\alpha_1 \leq \frac{\pi}{4} - \frac{\varphi}{2}, \tag{17}$$

Substituting a known value into this expression $\varphi = 25\text{-}30^0$ we get $\alpha_1 = 30\text{-}34^0$.

The height of the blade h is assumed to be equal to the minimum allowable height of the ridge H_1, т.е. h =100 mm.

With these parameters of the shaper's side dumps, a ridge with a height of at least 100 mm and a density of is formed on the field 1,0-1,2 r/sm^3.

Location of the irrigation hose on the ridge. The irrigation hose is laid on the ridge by water outlets above the soil surface and covered with a layer of soil, the angle of deviation from the axis of the water outlet to the soil surface should not exceed 15^0. The location of the irrigation hose is shown in Figure 9, where the cross section of the bed 1, irrigation hose 2, water outlet 3, trace 5 from the sealing roller of the seeder, soil layer 6 to cover the hose from solar radiation, contour 7 of the humidification zone, root system 8 of the plant, angle α of the deviation of the axis of the water outlet to the soil surface is schematically presented.

The irrigation hose is laid out in the field along the rows of plants on the ridge along the trail of the sealing pipe installed behind the comb shaper.

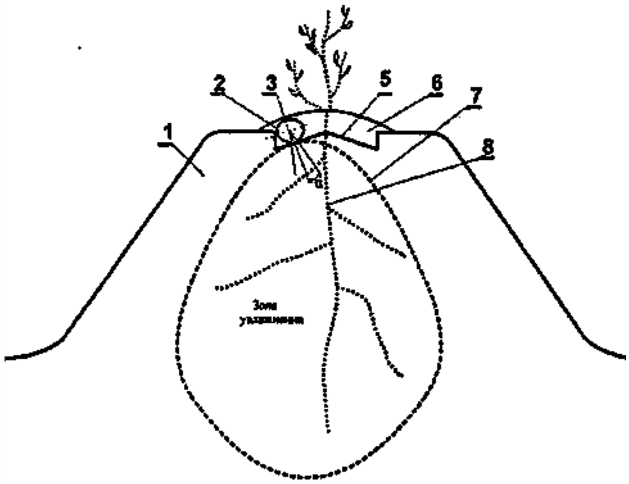

Figure 9. The scheme of laying the irrigation hose on the ridge.

Conclusions. 1) Based on the analysis of the weather conditions during the preparation and sowing of seeds, it was established that the minimum allowable height of the ridge H_1 must be at least 100 mm; minimum allowable width of the crest vertex $b_г$ from the point of view of stable operation of seeding devices should be at least 160 mm; permissible width of the lower base of the ridge $b_{oг}$ must be at least 435 mm. 2) Based on the analytical analysis, the parameters of the shaper are determined: the length of the shaper should be within L = 183–238,9 mm, and the width of the shaper's entrance apron B=292-334 mm, angle of installation of side dumps $\beta_y = 42 - 45^0$, height of the blade h equal to the minimum allowable height of the ridge H_1, i.e. h =100 mm. The density of the soil in the ridge is 1,0-1,2 g/sm^3. 3) With this method of drip irrigation, the heat content of the soil in the root system zone will be almost constant during the time of the day.

References.

1. Materials of the Uzhydromet on the daily amount of precipitation from March 25 to April 25 from 2008-2017, No. 25-01/532 of 09/15/2017.
2. Mamatov F, Mirzaev B, Berdimuratov P, Shaimardanov B. Aytmuratov M, Jumamuratov D Traction resistances of the cotton seeder moulder. GIS 2021 IOP Conf. Series: Earth and Environmental Science 868 (2021) 012052 IOP Publishing doi:10.1088/1755-1315/868/1/012052.
3. Berdimuratov P Development and justification of the parameters of the comb shaper for a cotton seeder. Disser. work for the degree of Doctor of Phil. Tech. sciences. (PhD). 2019. Tashkent.
4. Akhmetov A, The tendency to improve the design of cotton-growing pre-sowing tillage machines-tools. / Tashkent: ilmiy Akhborot technique - nashriyoti press 2017,. pp. 139-193.
5. Shaimardanov B, Shaimardanov H, Matchanov R. Irrigation hose for drip irrigation and the method of its installation. Patent UZ IAP 06314. 14.10.2020. (21). № IAP 2017 0013 № (22). 12.01.Tashkent. 2017.
6. Shaimardanov B Isakov A and Mirnigmatov B Methods of managing the agricultural background of cottonand technical means for their implementation CONMECHYDRO – 2020 IOP Conf. Series: Materials Science and Engineering (2020) 012153 IOP Publishing doi:10.1088/1757-899X/883/1/01215
7. Kurdyumov V Experimental study of a comb seeder equipped with combined coulters / V.I. Kurdyumov, E.S. Zykin, I.A. Sharonov // Bulletin of Saratov State Agrarian University named after N.I. Vavilov. Saratov, - 2012. - No. 11. pp.55-60.